

Geosphere

Initiation of Sierra Nevada range front–Walker Lane faulting ca. 12 Ma in the Ancestral Cascades arc

Cathy J. Busby, Jeanette C. Hagan and Paul Renne

Geosphere published online 14 August 2013;
doi: 10.1130/GES00927.1

Email alerting services

click www.gsapubs.org/cgi/alerts to receive free e-mail alerts when new articles cite this article

Subscribe

click www.gsapubs.org/subscriptions/ to subscribe to Geosphere

Permission request

click <http://www.geosociety.org/pubs/copyrt.htm#gsa> to contact GSA

Copyright not claimed on content prepared wholly by U.S. government employees within scope of their employment. Individual scientists are hereby granted permission, without fees or further requests to GSA, to use a single figure, a single table, and/or a brief paragraph of text in subsequent works and to make unlimited copies of items in GSA's journals for noncommercial use in classrooms to further education and science. This file may not be posted to any Web site, but authors may post the abstracts only of their articles on their own or their organization's Web site providing the posting includes a reference to the article's full citation. GSA provides this and other forums for the presentation of diverse opinions and positions by scientists worldwide, regardless of their race, citizenship, gender, religion, or political viewpoint. Opinions presented in this publication do not reflect official positions of the Society.

Notes

Advance online articles have been peer reviewed and accepted for publication but have not yet appeared in the paper journal (edited, typeset versions may be posted when available prior to final publication). Advance online articles are citable and establish publication priority; they are indexed by GeoRef from initial publication. Citations to Advance online articles must include the digital object identifier (DOIs) and date of initial publication.

Initiation of Sierra Nevada range front–Walker Lane faulting ca. 12 Ma in the Ancestral Cascades arc

Cathy J. Busby¹, Jeanette C. Hagan¹, and Paul Renne²

¹Department of Earth Science, University of California–Santa Barbara, Santa Barbara, California 93106, USA

²Berkeley Geochronology Center, 2455 Ridge Road, Berkeley, California 94709, USA

ABSTRACT

The eastern escarpment of the Sierra Nevada (USA) forms one of the most prominent topographic and geologic features in the Cordillera, yet the timing and nature of fault displacements along it remain relatively poorly known. The central Sierra Nevada range front is an ideal place to determine the structural evolution of the range front because it has abundant dateable Cenozoic volcanic rocks. The Sonora Pass area of the central Sierra Nevada is particularly good for reconstructing the slip history of range-front faults, because it includes unusually widespread and distinctive high-K volcanic rocks (the ca. 11.5–9 Ma Stanislaus Group) that serve as outstanding strain markers. These include the following, from base to top. (1) The Table Mountain Latite (TML) consists of voluminous trachyandesite, trachybasaltic andesite, and basalt lava flows, erupted from fault-controlled fissures in the Sierra Crest graben-vent system. (2) The Eureka Valley Tuff consists of three trachydacite ignimbrite members erupted from the Little Walker caldera. These ignimbrites are interstratified with lava flows that continued to erupt from the Sierra Crest graben-vent system, and include silicic high-K as well as intermediate to mafic high-K lavas. The graben-vent system consists of a single ~27-km-long, ~8–10-km-wide approximately north-south graben that is along the modern Sierran crest between Sonora Pass and Ebbetts Pass, with a series of approximately north-south half-grabens on its western margin, and an ~24-km-wide northeast transfer zone emanating from the northeast boundary of the graben on the modern range front south of Ebbetts Pass. In this paper we focus on the structural evolution of the Sonora Pass segment of the Sierra Nevada range front, which we do not include in the Sierra Crest

graben-vent complex because we have found no vents for high-K lava flows here. However, we show that these faults localized the high-K Little Walker caldera.

We demonstrate that the range-front faults at Sonora Pass were active before and during the ca. 11.5–9 Ma high-K volcanism. We show that these faults are dominantly approximately north-south down to the east normal faults, passing northward into a system of approximately northeast-southwest sinistral oblique normal faults that are on the southern end of the ~24-km-wide northeast transfer zone in the Sierra Crest graben-vent complex. At least half the slip on the north-south normal faults on the Sonora Pass range front occurred before and during eruption of the TML, prior to development of the Little Walker caldera. It has previously been suggested that the range-front faults formed a right-stepping transtensional stepover that controlled the siting of the Little Walker caldera; we support that interpretation by showing that synvolcanic throw on the faults increases southward toward the caldera. The Sonora Pass–Little Walker caldera area is shown here to be very similar in structural style and scale to the transtensional stepover at the Quaternary Long Valley field. Furthermore, the broader structural setting of both volcanic fields is similar, because both are associated with a major approximately northeast-southwest sinistral oblique normal fault zone. This structural style is typical of central Walker Lane belt transtension. Previous models have called for westward encroachment of Basin and Range extension into the Sierra Nevada range front after arc volcanism ceased (ca. 6–3.5 Ma); we show instead that Walker Lane transtension is responsible for the formation of the range front, and that it began by ca. 12 Ma. We conclude that Sierra Nevada range-front faulting at Sonora Pass initiated during high-K

arc volcanism, under a Walker Lane transtensional strain regime, and that this controlled the siting of the Little Walker caldera.

INTRODUCTION

The eastern escarpment of the Sierra Nevada (USA) is one of the most prominent topographic and geologic boundaries in the Cordillera (Surpless et al., 2002). The southern part of this boundary is relatively simple, straight and narrow along the southern Sierra Nevada range-front fault zone, but it becomes more complex in the central Sierra Nevada (between Mono Lake and Lake Tahoe; Fig. 1). There, it has been interpreted to form a northwest-trending zone of en echelon escarpments produced by normal or oblique faulting (Wakabayashi and Sawyer, 2001; Schweickert et al., 2004), with modern focal plane mechanisms suggestive of oblique normal faulting (Unruh et al., 2003). The long-term fault history of the southern Sierra Nevada escarpment is not well understood because Neogene volcanic rocks are generally lacking there, whereas the long-term history of the central part is more easily established and better understood due to the presence of Cenozoic volcanic and sedimentary rocks (Schweickert et al., 1999, 2000, 2004; Henry and Perkins, 2001; Surpless et al., 2002; Cashman et al., 2009). The central Sierra Nevada range front is an ideal place for determining the long-term history of the range-front faults because the area contains extensive dateable Cenozoic strata (Figs. 1, 2, and 3; Busby et al., 2008a, 2008b; Busby and Putirka, 2009; Hagan et al., 2009).

The Sonora Pass area is particularly advantageous for reconstructing the slip history of Sierra Nevada range-front faults, because the dateable Cenozoic volcanic strata include widely distributed, compositionally distinctive volcanic units; these are the high-K volcanic rocks of the Stanislaus Group (Fig. 2C) (for a detailed description of the stratigraphy, see Busby et al., 2013a).

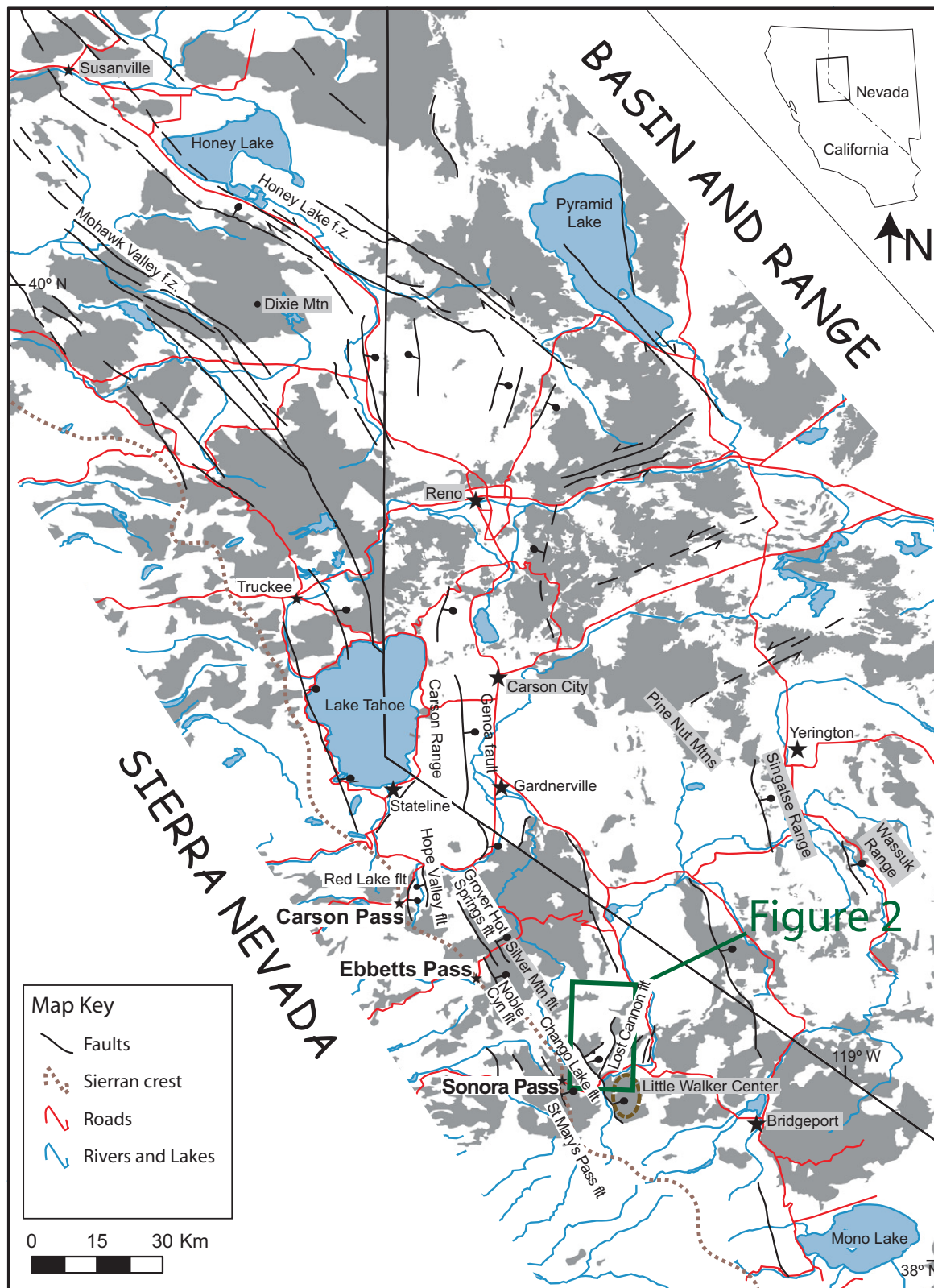


Figure 1. Faults of the central to northern Walker Lane belt, which has abundant Cenozoic volcanic rocks, shown in gray (all other rocks and sediments shown in white). F.z.—fault zone; flt—fault; Mtn—mountain. The brown dotted line represents the present-day Sierra Nevada range crest. Sources include Koenig (1963), Stewart and Carlson (1978), Wagner et al., (1981), Wagner and Saucedo (1992), Henry and Perkins (2001), Saucedo (2005), Busby et al. (2008a, 2008b), Hagan et al. (2009), and Cashman et al. (2009). Sierra Nevada range front at Sonora Pass is mapped in Figure 2.

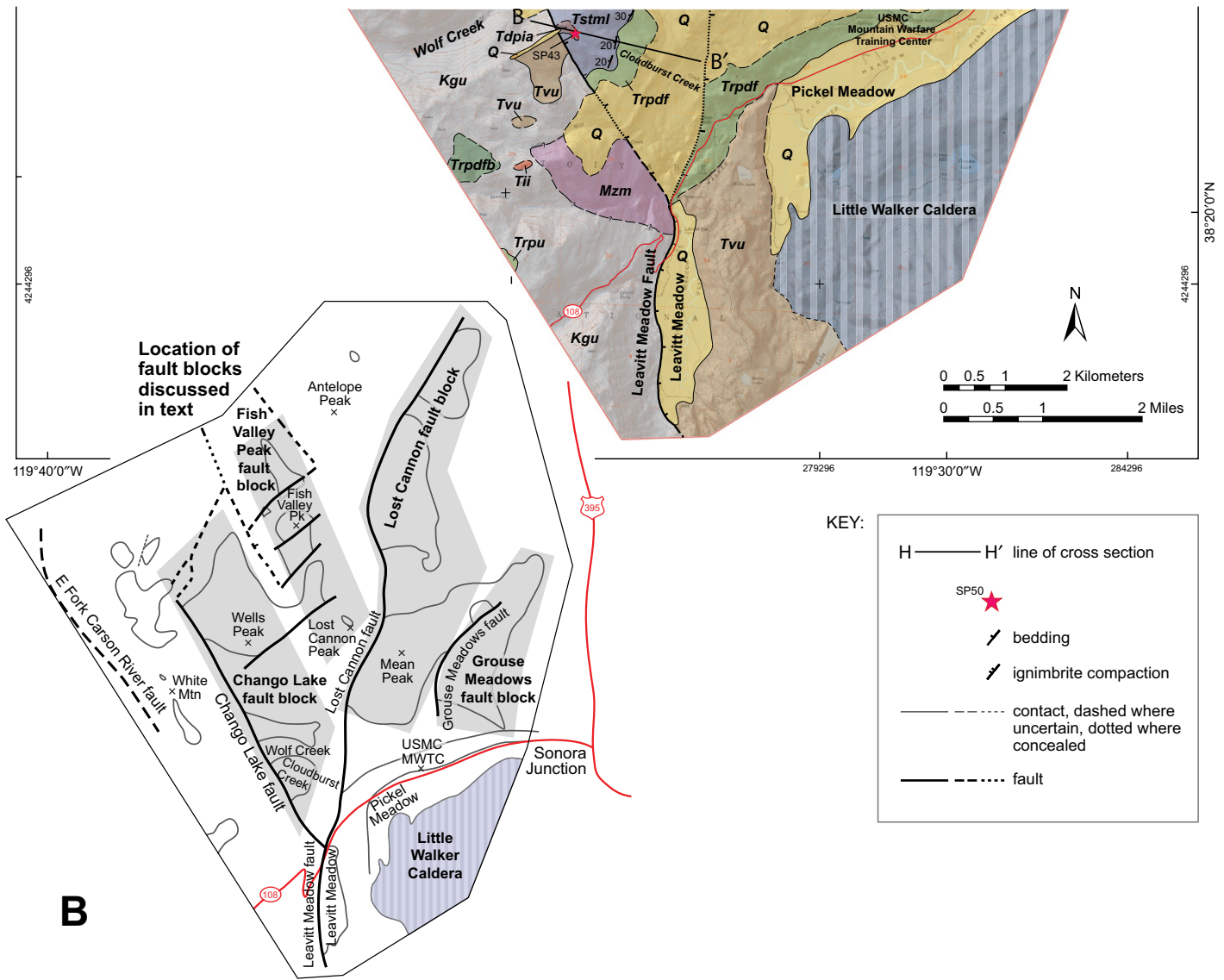


Figure 2 (continued).

tectonic depression. In contrast, the range-front half-grabens described herein lack associated vents; we describe them separately for that reason, and because they have been reactivated. In Busby et al. (2013a), the focus is more on the relationships between faults and vents in the Sierra Crest graben-vent system; here we focus on the structural evolution of the Sonora Pass segment of the Sierra Nevada range front.

Description of the faults in the central Sierra Nevada requires a discussion concerning the relative importance and timing of Basin and Range extension versus Walker Lane belt trans-tension in the region. The Walker Lane belt is a transtensional rift belt on the trailing edge of the Sierra Nevada microplate, and currently accommodates 20%–25% of the plate motion

between the North American and Pacific plates (see references in Putirka and Busby, 2011). The questions we address here are when did transtensional rifting begin, and what are the geologic signals of transtensional rift initiation?

PREVIOUS WORK AND GENERALIZED STRATIGRAPHY

Whitney (1880) and Lindgren and Knowlton (1911) recognized that Cenozoic strata in the broader region of the central and northern Sierra Nevada were deposited in westward-draining paleochannels cut into Mesozoic bedrock (unconformity 1; Fig. 2C). In the central Sierra Nevada, the oldest paleocanyon fill consists of Oligocene rhyolite ignimbrites, the Valley Springs Forma-

tion of Slemmons (1953; Fig. 2C). More recent work has shown that these ignimbrites erupted from calderas in central Nevada and flowed westward down paleochannels that cross the present-day Sierra Nevada and terminate in the Sacramento Valley of central California (Garside et al., 2005; Henry, 2008; Henry et al., 2012). Slemmons (1953) was the first to recognize that valleys were also cut into the Valley Springs Formation before the first andesites were deposited; recent work shows that this unconformity can be correlated across the Sierra Nevada, and is Early Miocene (unconformity 2; Fig. 2; Busby et al., 2008a, 2008b; Busby and Putirka, 2009; Hagan et al., 2009).

Middle Miocene andesitic volcanic and volcanoclastic rocks (Fig. 4A) that overlie the

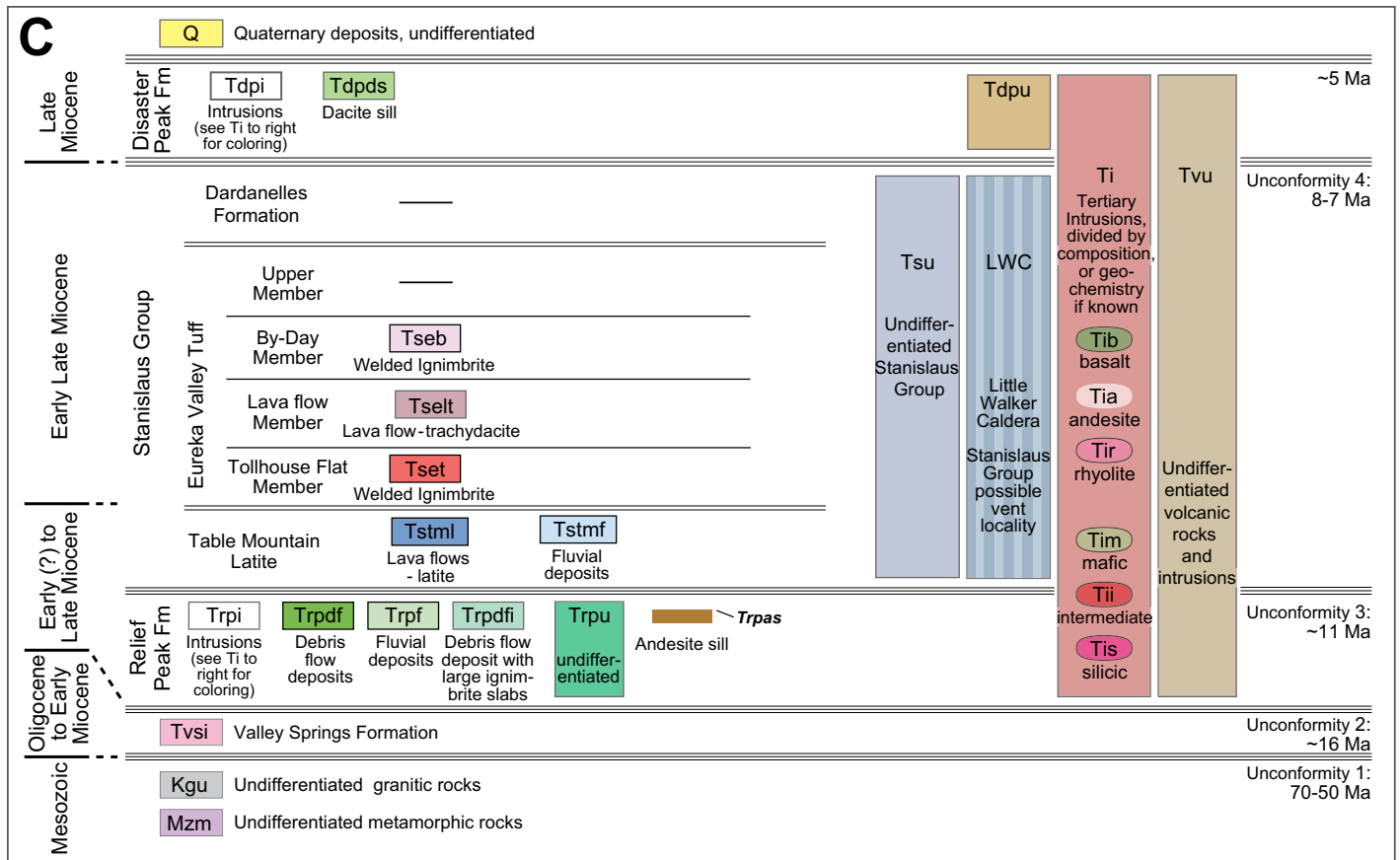


Figure 2 (continued).

Valley Springs Formation are referred to as Relief Peak Formation in the Sonora Pass region (Fig. 2; Slemmons, 1966). The Relief Peak Formation is separated from overlying high-K volcanic rocks of the Stanislaus Group by a third erosional unconformity recognized across the central Sierra (Fig. 2; Busby et al., 2008a, 2008b; Busby and Putirka, 2009; Hagan et al., 2009); at Sonora Pass, Slemmons (1953, p. 41) first identified this unconformity as the “prelatite erosion interval.” High-K volcanic rocks of the central Sierra Nevada were first described by Ransome (1898), who recognized their distinctive compositions and outcrop appearance (Figs. 4C, 4D) and referred to them as “latite” lava flows. Slemmons (1953) subsequently recognized that some of these latites are ash-flow tuffs (ignimbrites), now known as Tollhouse Flat Member, By-Day Member, and Upper Member of the Eureka Valley Tuff (formation status) of the Stanislaus Group (Fig. 2C). A fourth unconformity separates these rocks from overlying andesitic volcanic and volcanoclastic rocks of the Disaster Peak Formation (Busby et al., 2008a, 2008b, 2013a; Busby and Putirka, 2009; Hagan et al., 2009). Slemmons (1953,

1966) recognized the importance of range-front faults at Sonora Pass, but reported no evidence for synvolcanic faulting.

SIERRA NEVADA RANGE-FRONT HALF-GRABENS

We describe a series of four structural blocks along the Sierra Nevada range front (see Fig. 2B). Three of these, the Chango Lake, Lost Cannon, and Grouse Meadows fault blocks, form approximately north-northwest– to north-northeast–trending half-grabens that step down to the east. The very high, remote Fish Valley block is slightly less well understood, but is clearly cut by a set of northeast-striking faults (also mapped by Slemmons, 1953; Giusso, 1981).

As noted by Slemmons (1953), faults in the Sierra Nevada range front are rarely exposed because they generally coincident with valleys (Fig. 5). Many valleys in the central Sierra Nevada range front strike north-northwest or northeast, from Sonora Pass through Ebbetts Pass to Carson Pass; furthermore, offsets in Tertiary volcanic strata have been demonstrated across many of these north-northwest– and northeast-

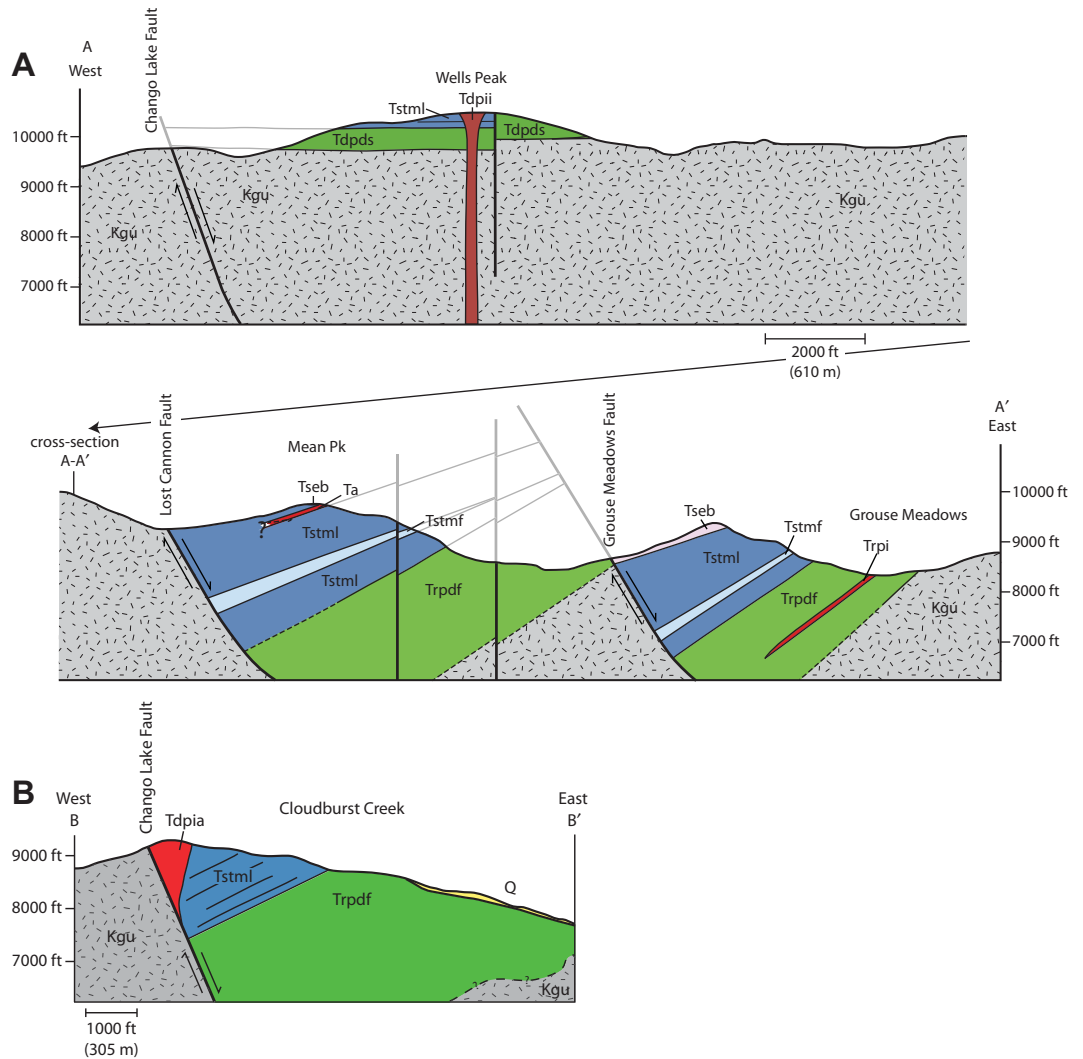
trending valleys (Curtis, 1951; Slemmons, 1953; Priest, 1979; Armin et al., 1983, 1984; Hagan et al., 2009; Hagan, 2010; Busby et al., 2013a). For the purposes of this paper, however, we show faults as inferred (with dashed lines) where we find long, straight, deep north-northwest– or northeast-trending valleys in granitic basement, but have no corroborating evidence in the form of offset of Cenozoic strata (e.g., see Silver King fault, Fish Valley fault, and Coyote Valley fault; Fig. 2; first mapped by Slemmons, 1953).

In the following, we first describe the stratigraphy of the fault block, including mineralogy, chemical composition, geochronology, and measured sections (Figs. 6, 7, 8, and 9), and then interpret the slip history of the fault.

Stratigraphy of the Chango Lake Fault Block

The Chango Lake fault block (see inset in Fig. 2) is defined by Cenozoic volcanic strata dropped down against granitic basement along the Chango Lake fault. These strata are preserved in two areas, Wells Peak to the north, and Cloudburst Creek to the south (Fig. 2).

Figure 3 (on this and following page). Structure sections through Miocene volcanic strata in the Sonora Pass range front, by (Hagan, 2010; modifications by C. Busby). Locations are plotted in Figures 2A and 2B, and map units are given in Figure 2C. (A) A–A': cross section west to east through the Chango Lake normal fault, an unnamed fault, the Lost Cannon normal fault, and the Grouse Meadows normal fault. The Relief Peak Formation and the TML lava flows crop out at lower elevations in each successive fault block; amount of displacement discussed in the text. (B) B–B': cross section west to east through the Chango Lake fault at Cloudburst Creek. An andesite plug (Tdpia) intrudes the Table Mountain Latite (TML) lava flows (Tstml) along the fault.



Wells Peak Section

The Wells Peak section overlies granitic basement and dips ~5°–11° northwest (Figs. 2 and 3). The basal part of this section has not been accessed on the north side, where it is mapped by air photo as undifferentiated Relief Peak Formation beneath TML (Trpu; Fig. 2). However, we have mapped and sampled the south part of the section, which consists of a dacite with plagioclase and quartz (sample SP-25; Figs. 6, 7, and 8; Tables 1 and 2). This dacite was previously considered to be a lava flow (Hagan, 2010), but its age is too young (6.5 ± 0.2 Ma; Fig. 8D) for it to be an extrusive rock beneath the TML. We here reinterpret it as a dacite sill and group it with the Disaster Peak Formation (Tdpds; Fig. 2), as indicated by its age, and the following field features: low aspect ratio, laterally uniform thickness, and lack of flow breccias in outcrop or within float, all of which are atypical of silicic lava flows. In addition, this mass has extremely uniform

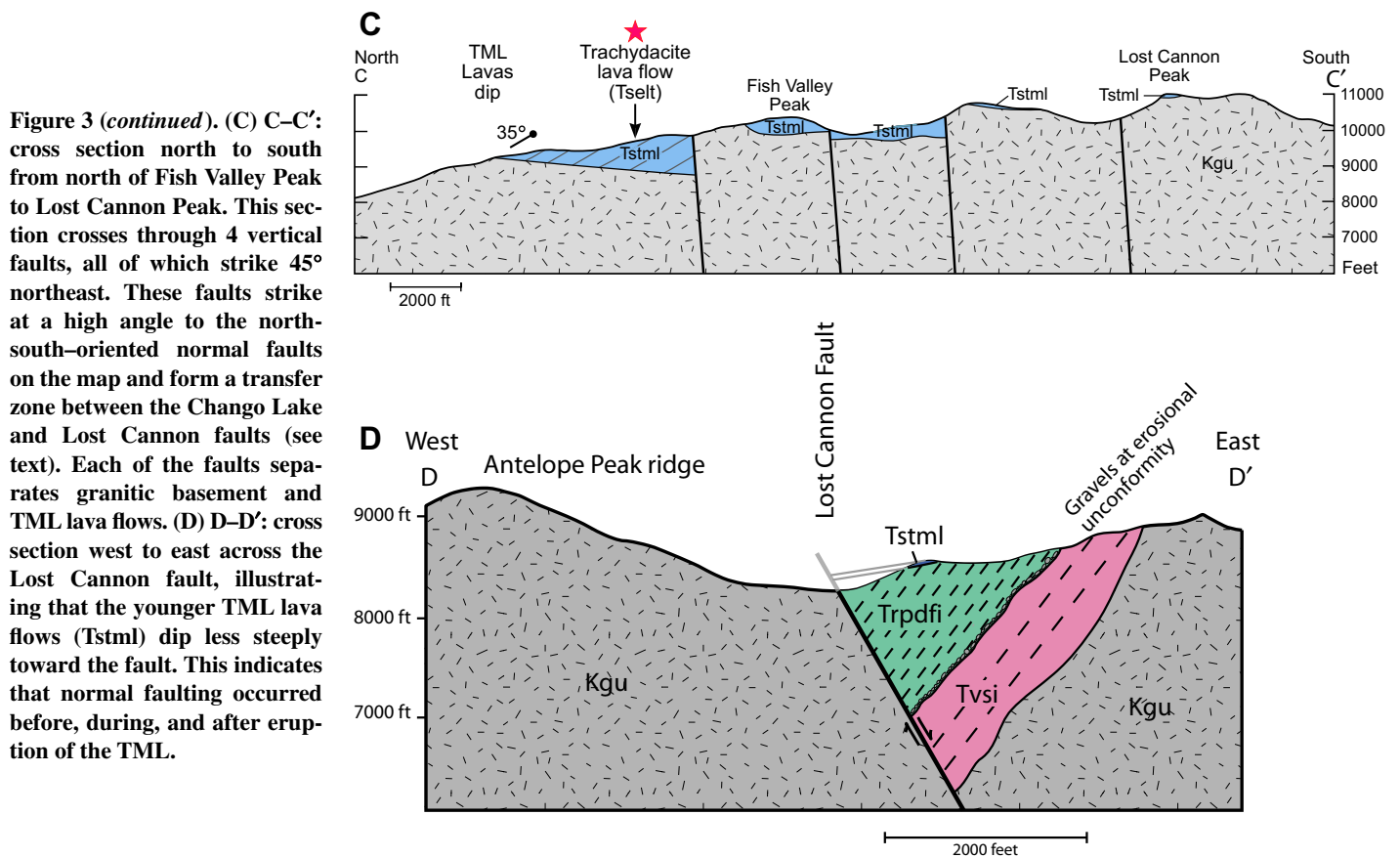
horizontal flow banding throughout (parallel to upper and lower contacts), which is typical of sills but not silicic lava flows (which typically have chaotic flow banding). Hagan (2010) also reported 14% sanidine in this unit, but in fact the unit only contains plagioclase feldspar, which was dated (Fig. 8C). Having identified this mass as an intrusion and not a lava flow, we can report that there are no primary volcanic rocks in the Relief Peak Formation in the range-front half-grabens mapped in Figure 2, although they occur to the west, in the Sierra Crest graben-vent system (Busby et al., 2013a) and the Cataract paleochannel fill to the west of that (Koerner, 2010), both shown in Figure 10. We assume that vent deposits for the Relief Peak Formation are in the same general area as the Stanislaus Group vents deposits shown in Figure 10, but the latter are far more obvious because of their volume.

The Wells Peak section includes a 140–230-m-thick section of TML lava flows (top

eroded); the uppermost flow contains the coarsest sieve-texture plagioclase and pyroxene phenocrysts. Some flows are separated by <1-m-thick pebbly sandstone to cobbly sandstone beds. The top of Wells Peak is formed of an elongate plug of intermediate composition (Tdpia; Fig. 2).

The remnants of a basaltic plug, surrounded by an unconsolidated deposit of basalt scoria and bombs, intrude and overlie the TML ~1.8 km north of Wells Peak (Tdpib; Fig. 2; see photos in Figs. 4E, 4F). These are the only strata that are younger than the Stanislaus Group in the segment of the range front shown in Figure 2; all other units younger than Stanislaus Group are intrusions. The plug is composed of crystal-rich basalt that contains fine-grained rounded olivine crystals, and euhedral plagioclase, clinopyroxene, and orthopyroxene phenocrysts (sample JHSP-29; Figs. 6 and 7; Tables 1 and 2). We attempted to date plagioclase from this unit by the $^{40}\text{Ar}/^{39}\text{Ar}$ method but obtained an integrated

Sierra Nevada range front–Walker Lane faulting in the Ancestral Cascades arc



age of 23.48 ± 0.12 Ma (Fig. 8D), which we interpret to reflect inherited plagioclase xenocrysts. The age spectrum for this sample suggests a magmatic age younger than 10 Ma, as indicated by the initial heating steps.

Cloudburst Creek Section

Cenozoic volcanic rocks are covered by morainal debris along Wolf Creek and Silver Creek Meadows, but one section of TML is exposed on the ridge north of Wolf Creek, and the TML and underlying Relief Peak Formation are exposed on a ridge at the head of Cloudburst Creek (Fig. 2). The ridge of TML north of Wolf Creek was previously mapped as moraine by Giusso (1981), while the section at Cloudburst Creek was mapped solely as Relief Peak Formation by Giusso (1981) and mapped solely as TML by D.B. Slemmons (unpublished map provided by the California Geological Survey), but both formations are present (Fig. 2). Only ~50–60 m of Relief Peak Formation andesitic debris flow deposits are exposed beneath the TML at Cloudburst Creek, but to the east, these deposits reemerge from beneath the moraine and form extensive outcrops north of Pickel Meadow (Fig. 2), and thus are inferred to be very thick (Fig. 3B).

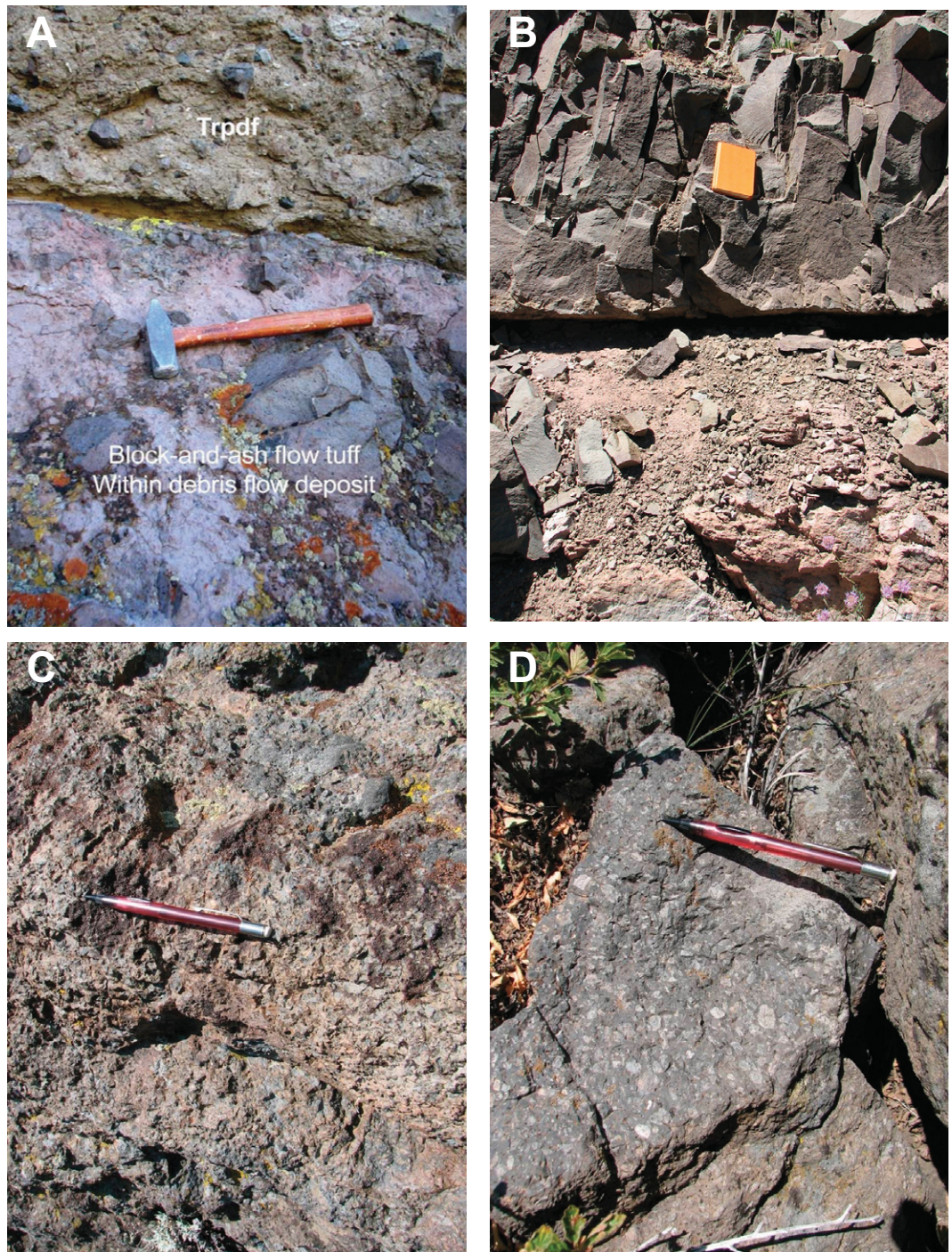
TML lava flows at both Wolf Creek and Cloudburst Creek dip westward $\sim 20^\circ$ – 30° toward the Chango Lake fault (Figs. 3B and 5D). A measured section through the Cloudburst Creek section (Fig. 9A) shows that the >410 -m-thick (top eroded) latite section contains 20 flows, many separated by flow-top breccias, similar to other TML volcanic sections (Busby et al., 2008a). Vesicles are common in the top of the coherent zones, and elongated vesicles have a north-south preferred elongation, parallel to the strike of the half-graben, and perpendicular to the regional paleochannels. Flow 19 has reversed magnetic polarity, whereas all of the other flows in this section have normal polarity (C. Pluhar, 2012, written commun.). The reversed polarity flow may thus either correspond to flow 14 (classic TML) or flow 19 of the Sonora Peak section, which are both reversely polarized (Busby et al., 2008a; Pluhar et al., 2009; C. Pluhar, 2012, written commun.).

A small plug emplaced along the Chango Lake fault intrudes the eroded top of the TML section (Tdpia; Figs. 2 and 3B); its composition is on the boundary between andesite and basaltic andesite (sample 43; Fig. 7), and it contains plagioclase and oxidized hornblende phenocrysts.

Chango Lake Fault

The long northwest-trending fault that extends past Chango Lake was mapped by Slemmons (1953), who named it the Silver King fault. However, we map the short fault in Silver King Creek as the Silver King fault, one of several northeast-striking transfer faults, and herein name the long northwest-trending fault the Chango Lake fault, after the lake whose position appears to be a geomorphic expression of the fault (Fig. 2). Slemmons (1953) also mapped the long, north-northeast-striking Lost Cannon fault to the east, and inferred that these two long faults are beneath moraines and continue south as the Leavitt Meadows fault (as shown in our map; Fig. 2). Slemmons (1953) showed the north end of the north-northwest-striking Chango Lake fault turning sharply toward the northeast, extending down Silver King Canyon along a non-linear trace, and ending at a fault he mapped in Fish Valley–Four Mile Canyon (Fig. 2). We show these faults with a dashed line, because we cannot demonstrate that they offset Cenozoic volcanic units. The Chango Lake fault strikes $\sim 330^\circ$, but its dip is not directly observable in outcrop. The fault has a linear surface trace for >10 km, and cuts across steep topography, so it must

Figure 4 (on this and following page). Outcrop photos from the Sierra Nevada range front at Sonora Pass. Rock unit abbreviations are in Figure 2C. (A) The Relief Peak Formation in this area includes extremely little primary volcanic rock, and is composed mainly of volcanic debris flow deposits, some containing slabs and blocks of remobilized primary volcanic rock. Part of an ~20 m block of block-and-ash flow tuff, enclosed in a debris flow deposit, is shown. (B) The basal contact of an andesite sill that intrudes the Relief Peak Formation (see measured section in Fig. 9B). The sill forms columnar joints against the underlying contact with Relief Peak Formation debris flow deposits (field notebook for scale). The sill is included with the Relief Peak Formation in Figure 2 (Trpas) on the basis of its $^{40}\text{Ar}/^{39}\text{Ar}$ hornblende age (12.15 ± 0.04 , see sample SP-50 in Fig. 8B; modal analyses and geochemistry in Figs. 6 and 7). (C) Distinctive weathering pattern of Table Mountain Latite (TML), created by weathering of stretched vesicles and large plagioclase phenocrysts. (D) A typical fresh outcrop of TML, with large skeletal plagioclase phenocrysts.



dip steeply ($>70^\circ$ east). Because the fault is so straight (Fig. 2), displacement along its trace may include a strike-slip component, but no piercing points are identifiable to test this idea. Chango Lake is at the western edge of a topographic flat in the hanging wall of the fault, against the fault (Fig. 2); this geomorphic feature may indicate that the fault has been active in postglacial time.

At its north end, the Chango Lake fault drops the base of the TML down to the east, from

White Mountain in the footwall, to the Wells Peak section in the hanging wall (Fig. 2); this constitutes ~182 m of vertical displacement. White Mountain forms a horst block between the Chango Lake fault to the east (Fig. 2) and the East Fork Carson fault to the west (mapped by Busby et al., 2013a; also see Fig. 10). The Relief Peak Formation is missing on the horst block (Fig. 2), and present as avalanche deposits as much as 1.6 km thick on the hanging wall of

the East Fork Carson fault; thus we infer that the Relief Peak Formation was stripped from the horst block by avalanching before the TML was erupted (Busby et al., 2013a). The dacite sill (Tdpds) appears to emanate from the Chango lake fault into its hanging-wall strata, suggesting that the fault acted as a conduit for it.

Farther south, in the Cloudburst Creek area (Fig. 2B), the base of the TML is offset at least 550 m from the White Mountain horst block

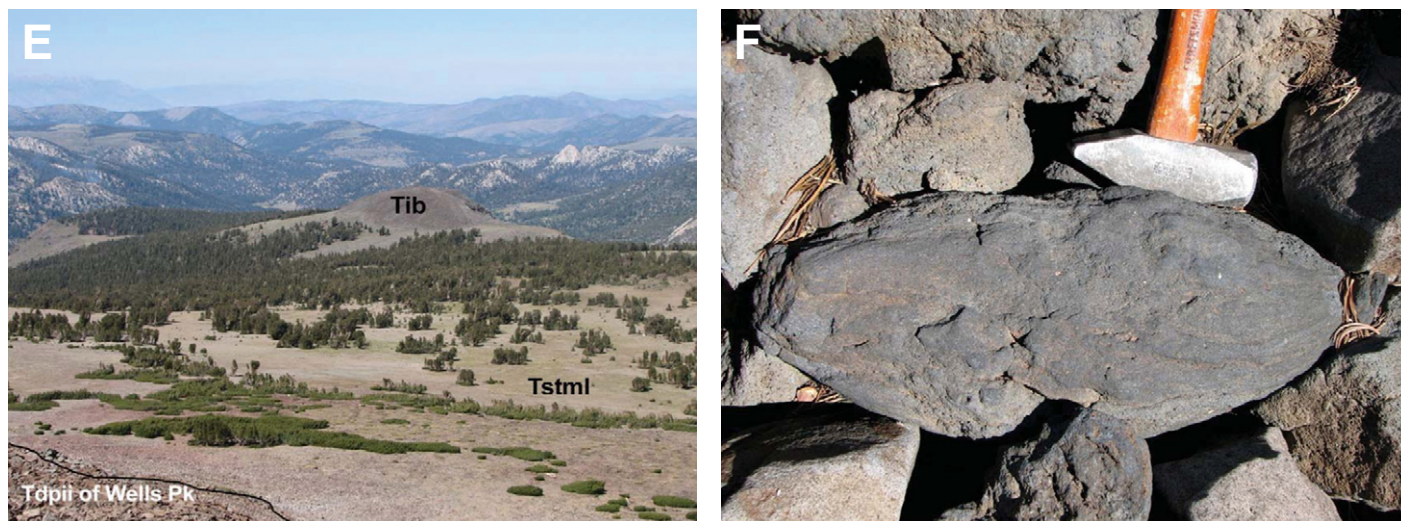


Figure 4 (continued). (E) View of an olivine two-pyroxene basalt cinder cone (modal analyses and geochemistry in Figs. 6 and 7), on the bench formed by TML at Wells Peak (see Fig. 2A). Like many of the peaks in the region, Wells Peak was formed by an intrusion (Tdpil, Disaster Peak intrusion of intermediate composition) that baked the surrounding rocks. Cone labeled “Tib” is about 70 m high. (F) Loose volcanic bombs on the surface of the basaltic cinder cone shown in E, indicating an extremely young age. However, $^{40}\text{Ar}/^{39}\text{Ar}$ dating failed to constrain its age (plagioclase inherited integrated age of 23.48 ± 0.12 Ma; Fig. 8D).

(Fig. 3B). Consequently, displacement increases southward, which is consistent with the fact that stratal dips in the half-graben increase southward (cf. Figs. 3A, 3B). Alternatively, these relations may result from an increase in fault curvature, which seems unlikely, given its very straight trace.

Stratigraphy and Structure of the Fish Valley Peak Block

The Fish Valley Peak block is bounded on the southwest by the Fish Valley fault, on the northeast by the Coyote Valley fault, and on the southeast by the Lost Cannon fault (see Fig. 2B); all three of these faults were mapped by Slemmons (1953). In the Fish Valley Peak block, TML lava flows (Tstml) directly overlie granitic basement and are cut by four subvertical faults that strike northeast, referred to here as the Fish Valley Peak fault zone (see also Figs. 2, 3C, and 10). The southernmost of these faults (immediately north of Lost Cannon Peak; Figs. 2A and 3C) places the TML against granitic basement; viewed from the Wells Peak ridge to the southwest, the fault surface appears to dip $\sim 70^\circ$ southeast (Fig. 5E), which would make it a reverse fault, but that is an artifact of the perspective; the fault is steep (Fig. 3C), and it offsets the contact between the TML and the dacite sill (Tdpds) in apparent sinistral sense (Fig. 2A). Within the northernmost block along the Fish Valley Peak ridge, good exposure of TML lava flows shows that they dip $\sim 35^\circ$ to $\sim 22^\circ$ toward the northwest (Figs. 2 and 3C), suggesting

that they were dropped down to the east along the Fish Valley fault after deposition. In cross section (Fig. 3C) these flows appear to downlap onto granitic basement, but we do not see downlap of the TML onto basement anywhere else; it always is parallel to the depositional surface, suggesting that the flows were not viscous enough to form edifices with any appreciable surface slope on them. Instead, we infer that the lavas were deposited flat against a granitic high, which they overlapped, and that this contact and strata contained within this block were rotated $\sim 35^\circ$ toward the northwest, after TML deposition (Figs. 2 and 3C). Consequently, the northeast faults formed as down to the northwest normal faults, with initial dips of $\sim 20^\circ$ to the northwest, which then became rotated by down to the east slip on the Fish Valley fault, so they appear to be high-angle reverse faults in cross section. As such, the northeast faults are oblique sinistral normal faults.

The northeast-striking Fish Valley Peak faults may extend further to the east than shown in Figure 2, but they are difficult to trace through the granitic basement. For example, the northeast end of the southernmost northeast fault may curve down a northeast-trending valley visible in the granite on the digital elevation model (Fig. 2), and merge with the Lost Cannon fault. Regardless of their length, the Fish Valley Peak faults appear to transfer displacement between the Fish Valley and Coyote Valley faults; or, taking a broader view, they transfer motion from the Chango Lake fault to the Lost Cannon fault (Fig. 2). The Fish Valley Peak fault zone is the

southernmost northeast transfer fault zone of a series that extends down the range front northward to Ebbetts Pass (e.g., see Poison Flat–Mineral Mountain, Falls–Meadow–Dumont Meadows, and Jones Canyon faults in fig. 11 of Busby et al., 2013a).

In addition to TML flows, the Fish Valley Peak block contains a very small (90 m diameter) erosional remnant of trachydacite lava flow on the TML (Tselt; Fig. 2; sample JHSP-27; Fig. 7). This was assigned to the Eureka Valley Tuff (EVT) Lava Flow Member in Hagan (2010), even though no Tollhouse Flat Member intervenes, because (1) the TML lacks silicic volcanic rocks elsewhere, and (2) the EVT Lava Flow Member has them in the type section of the Stanislaus Group (Koerner et al., 2009). This lava flow has very sparse, red-brown oxidized phenocrysts, similar to those at the type section where the red Fe-oxide pseudomorphs are preserved well enough to identify them as hornblende (Koerner et al., 2009). However, in the Poison Flat transfer zone north of our study area (see fig. 11 of Busby et al., 2013a), we have dated a similar trachydacite that intrudes the TML and passes upward into a lava flow that overlies the TML. A $^{40}\text{Ar}/^{39}\text{Ar}$ hornblende age on that trachydacite (Busby et al., 2013b) is intermediate in age between the EVT Tollhouse Flat Member (9.54 ± 0.04) and the youngest age obtained so far on the TML (10.36 ± 0.06). Accordingly, not all silicic high-K lava flows in this region and general time period can be assigned to the EVT Lava Flow Member. In addition, recent work in the type section by Chris Pluhar et al.



Grouse Meadow area

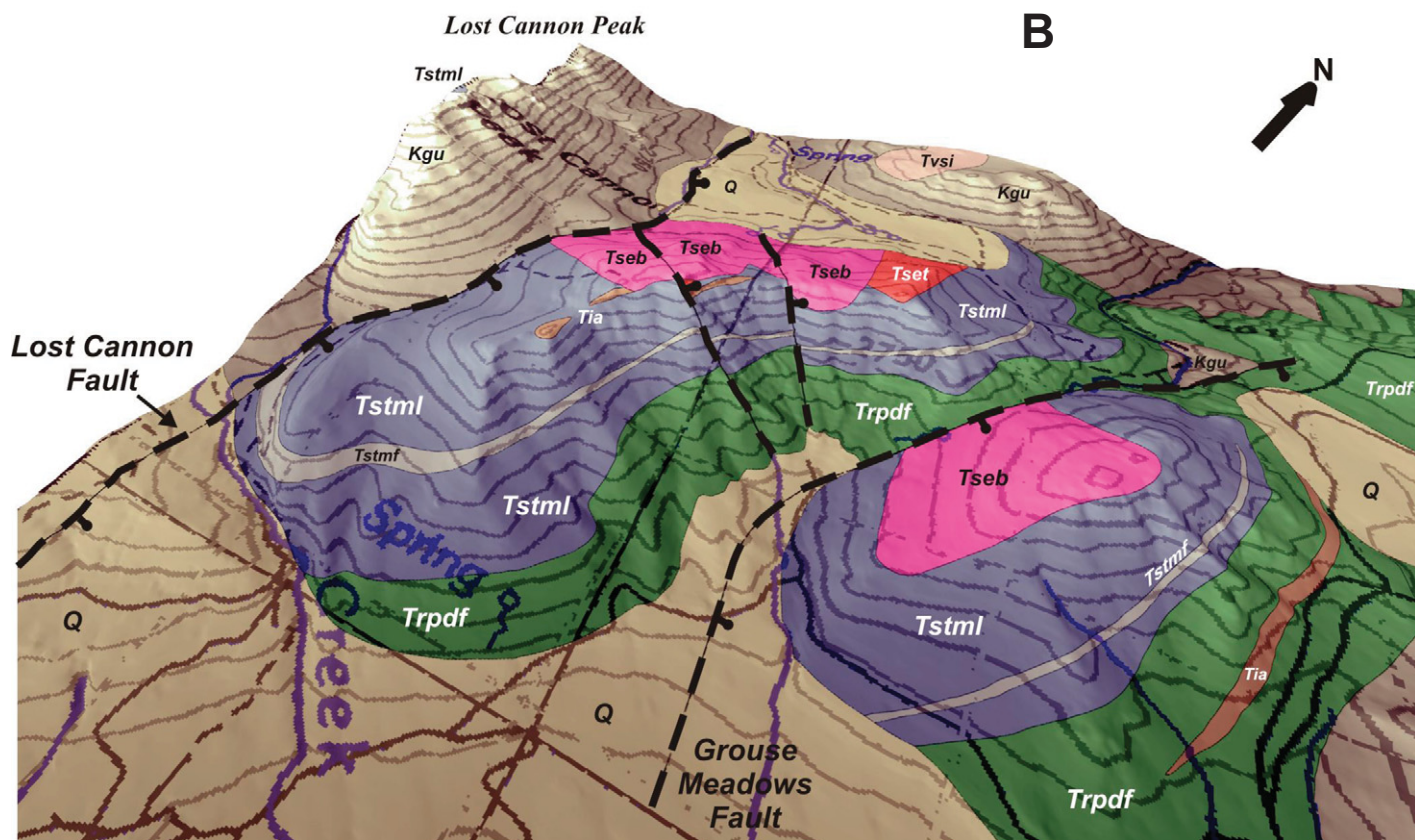


Figure 5 (on this and following two pages). Views of faults in the Sierra Nevada range front at Sonora Pass. Rock unit abbreviations are in Figure 2C. (A) Oblique areal view. (B) Geologic map interpretation of A, the fault blocks tilted westward toward the Grouse Meadows fault and the Lost Cannon fault. Lost Cannon Peak in distance is the highest peak on the range front at Sonora Pass, and consists of granitic basement uplifted in the footwall on the Lost Cannon fault. The oblique map view also illustrates the paleotopography that existed before extension began, created by carving of paleochannels into Mesozoic granitic bedrock. For example, Miocene strata in both fault blocks end abruptly against a paleochannel wall, rather than ending against faults. This complication makes it more difficult to accurately estimate offset on the faults.

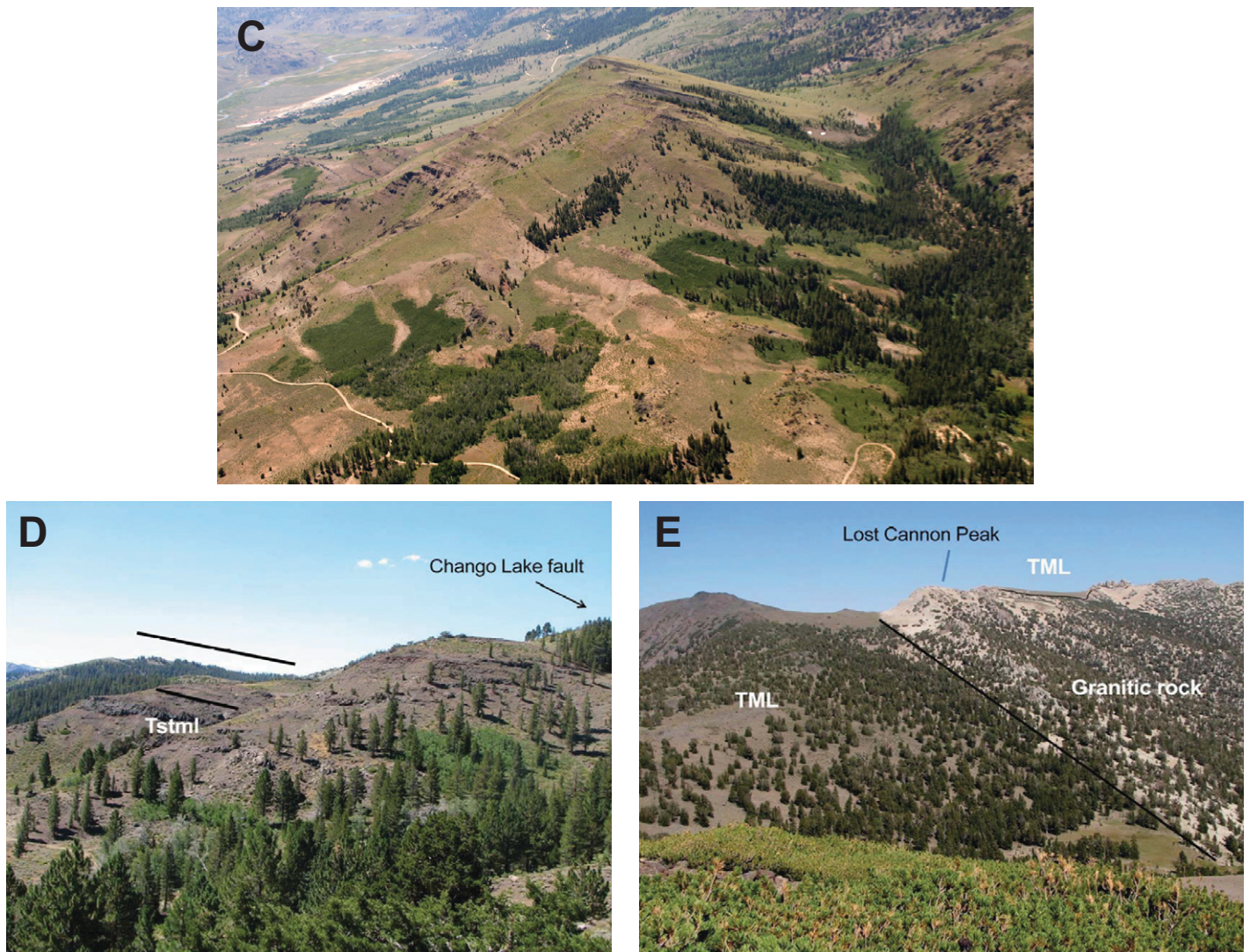
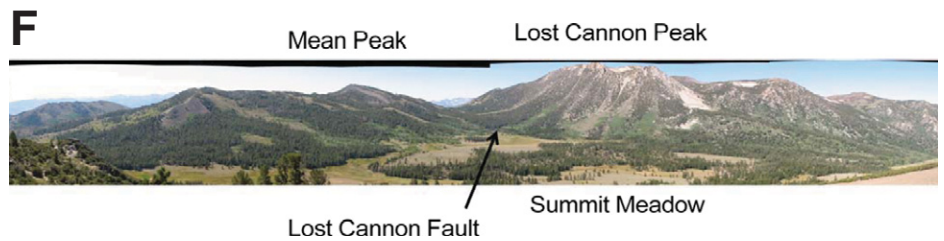


Figure 5 (*continued*). (C) A view from the north shows the prominent valleys that follow the Grouse Meadows fault (valley with trees in right foreground) and the Leavitt Meadow fault (with meandering stream in left distance). Because faults commonly form valleys in the range front, they are very rarely exposed (e.g., see Hagan et al., 2009), making it difficult to gather kinematic data. The poor stratification in Relief Peak Formation debris flow deposits (Fig. 9B), visible at the level of the road (left side of photo), and slightly irregular layering of Table Mountain Latite (TML) lava flows (prominent outcrops in upper half of section) make estimation of dips slightly imprecise, but compaction fabrics in the welded ignimbrites of the Eureka Valley tuff are extremely consistent (By-Day Member shown here; black rocks at top of section forming dip slope slanting down toward Grouse Meadows fault). Despite this irregularity (shown in Fig. 2), dips appear to flatten upward in the section, from $\sim 40^\circ$ to $\sim 20^\circ$. Faulting during deposition of the section is further indicated by thickening of the fluvial interbed in TML toward the Lost Canyon fault (shown as Tstml in Fig. 2). (D) View of Cloudburst Creek section (see measured section in Fig. 9A). The TML lava flows dip 25° west toward the Chango Lake fault (not visible at right of photo; see cross section in Fig. 3B). (E) View of northeast-striking, vertical transfer fault with apparent left-lateral displacement, taken from Wells Peak looking westward toward Lost Cannon Peak (see Fig. 2). The perspective makes the fault appear to be a reverse fault, but it is vertical. The fault places the TML against granitic rocks of Lost Cannon Peak. Note that the TML directly overlies granitic basement at Lost Cannon Peak (see TML in photo), which is in the footwall of the Lost Cannon fault; in contrast, in the hanging wall of the Lost Cannon fault, it is underlain by a thick section of Relief Peak Formation (see Fig. 2).

Busby et al.

Figure 5 (continued). (F) View of Lost Cannon fault, looking south toward Summit Meadow (see Fig. 2). The dark colored rocks on the left (east) are Miocene volcanic rocks, dropped down against granitic rocks of Lost Cannon Peak along the Lost Cannon fault. The higher ridges of Mean Peak are held up by TML flows, and the lower slope (to the left) is composed of less resistant Relief Peak debris flow deposits. The dip slope that extends from Mean Peak toward the fault consists of welded ignimbrite of the Eureka Valley Tuff (By-Day Member Tseb; Fig. 2) similar to the dip slope in the hanging wall of the Grouse Meadows fault, shown in C.



(2012, written commun.) identified a trachydacite lava flow between the TML and Tollhouse Flat Member; he groups this lava flow with the EVT because the TML has no silicic flows, referring to it as EVT Basal Lava Flow Member. Thus, the undated trachydacite lava flow on Fish Valley Peak ridge could be either EVT Lava Flow Member or EVT Basal Lava Flow Member. The dated trachydacite intrusion and lava

flow in the Poison Flat fault zone is important because it demonstrates that Stanislaus Group magmas vented along a range-front transfer fault zone in that area. The undated silicic lava flow in the Fish Valley Peak transfer zone is important because most flows of this composition are viscous and not laterally extensive, which suggests that the isolated outcrop at JHSP-27 may have vented from the Fish Valley Peak transfer zone

(Fig. 2). The occurrence of the trachydacite flow on top of tilted TML lavas suggests that the TML was tilted before the trachydacite was erupted. A similar amount of post-TML, pre-EVT tilting is inferred for the Arnot Creek fault on the west side of the Sierra Crest graben (see fig. 11A of Busby et al., 2013a).

The four northeast sinistral oblique normal faults of the Fish Valley Peak fault zone form

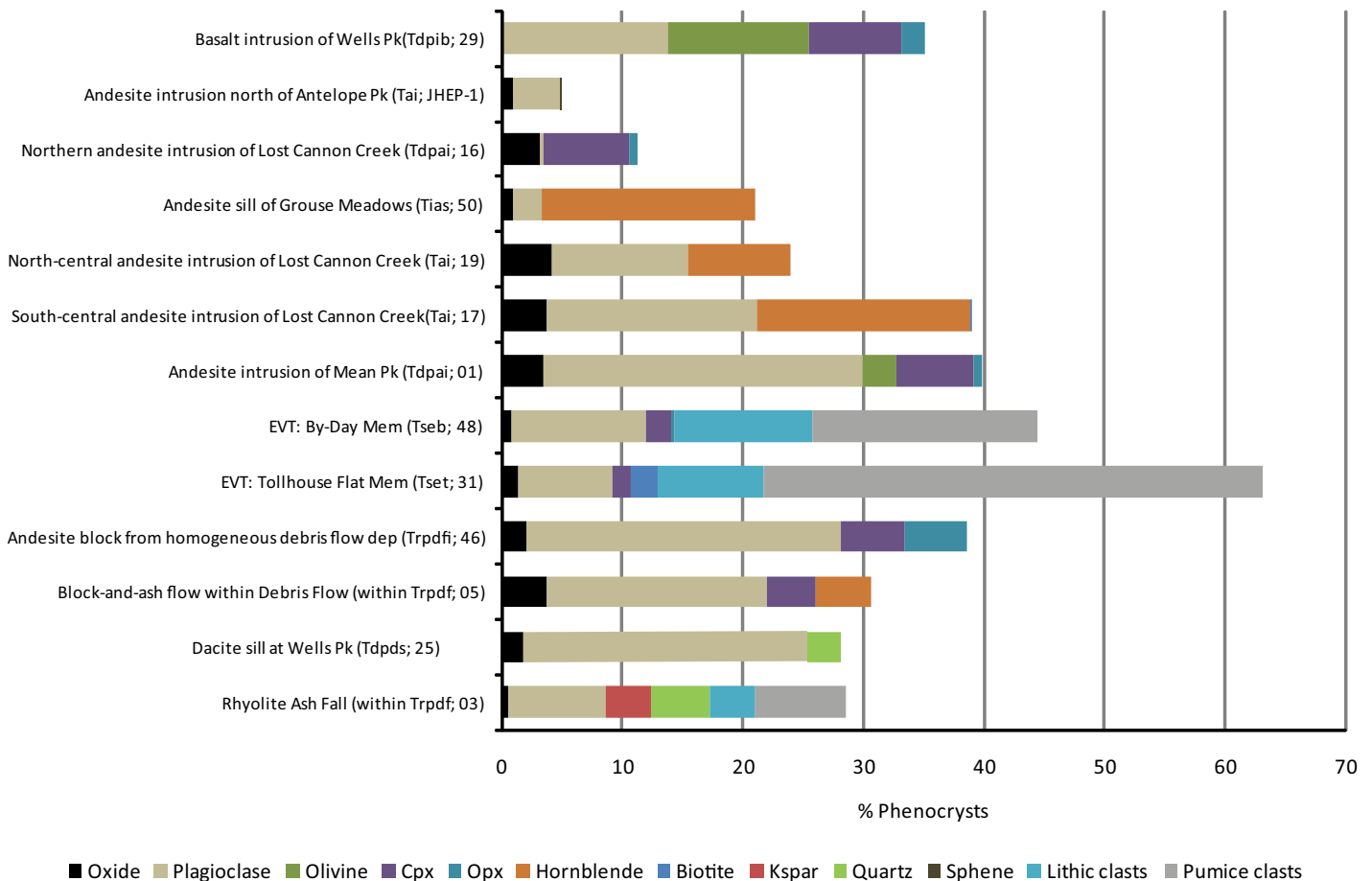


Figure 6. Modal analyses of 13 volcanic and subvolcanic rock samples from the area mapped in Figure 2 (samples plotted there), grouped by formation and arranged in stratigraphic order (Pk—peak; Mem—member; EVT—Eureka Valley Tuff; Cpx—clinopyroxene; Opx—orthopyroxene; Kspar—potassium feldspar). Groundmass, altered crystals, and volcanic glass compose the rest of the rock (Table 1). Sample numbers are given.

the southern edge of a 25-km-wide northeast transfer zone (described in Busby et al., 2013a); this major transfer zone is important for demonstrating that the synvolcanic structures are an integral component of the central Walker Lane (Busby et al., 2013b).

Stratigraphy of the Grouse Meadows Fault Block

The Lost Cannon fault block is west of the Grouse Meadows fault block (see Fig. 2B), described here because its stratigraphy is more complete and a basal contact on basement is preserved; a description of the largely repeated stratigraphy in the Lost Cannon fault block follows. Oblique air photos and oblique geologic map views of the Grouse Meadows and Lost Cannon fault blocks are shown in Figures 5A–5C.

West-tilted strata of the Grouse Meadows fault block were first mapped by Priest (1979), but his map did not extend west to the east-dipping Grouse Meadows fault, mapped here for the first time (Fig. 2). Dips range from 39° in basal strata Relief Peak Formation strata, to 28° in the upper part of TML, to 20° in the EVT (Fig. 2), suggesting tilting during deposition of the half-graben fill.

The Relief Peak Formation in the Grouse Meadows block (Trpdf; Fig. 2) consists of andesitic debris flow deposits with abundant megablocks of Valley Springs Formation, especially at its base (mapped as debris flow deposits with ignimbrite slabs, Trpdf; Fig. 2). Megablocks of andesitic block-and-ash-flow tuff and mafic flow breccia occur throughout the Relief Peak Formation debris flow deposits (Trpdf), but are less abundant. An ~30-m-long Valley Springs Formation megablock near the base of the section was mapped by Priest (1979) as in situ Valley Spring Formation, but it clearly is above the basal contact with the granitic basement where it is surrounded by Relief Peak Formation andesitic debris flow deposits. The Valley Springs Formation megablocks range from nonwelded ignimbrites, which were relatively soft when emplaced as megablocks, to densely welded varieties that were rigid enough to become thoroughly shattered by the avalanching process (e.g., see shattering of avalanche blocks described by Takarada et al., 1999). A 4 by 4 m megablock of block-and-ash-flow tuff (Busby and Wagner, 2006) is particularly well exposed uphill and upsection from a prominent sill (Tias; Fig. 2); the block-and-ash-flow tuff is a plagioclase hornblende clinopyroxene basaltic andesite (sample JHSP-5; Figs. 6 and 7; Tables 1 and 2). Landslide blocks are also abundant in the Relief Peak Formation in the hanging wall of the Lost Cannon fault (Trpdf; Fig. 2,

described in the following). The Valley Springs Formation megablocks record landsliding of lithified paleochannel fill deposits from horst blocks into the half-grabens prior to eruption of the TML (note that in situ Valley Springs Formation paleochannel fill is preserved at the base of the northern part of the Lost Cannon half-graben, described in the following). Any Relief Peak Formation debris flow paleochannel fill that originally was on the horst block evidently was not lithified, because there are no debris flow megablocks within the range-front grabens (as would be shown by chaotic dips, like those that predominate in the Relief Peak Formation in the Sierra Crest graben; Busby et al., 2013a). The debris flow deposits generally lack stratification (as shown in measured section; Fig. 9B), and lack fluvial interbeds except in the uppermost part of the formation in the Grouse Meadows (stratified pebbly sandstones; Busby and Wagner, 2006; not mapped separately in Fig. 2).

These features suggest catastrophic deposition, perhaps by resedimentation of unconsolidated debris flows from horst blocks into grabens.

A remarkably concordant hornblende plagioclase andesite sill intrudes the Relief Peak Formation within the Grouse Meadows fault block (Trpas; Fig. 2; sample JHSP-50; Figs. 6 and 7; Tables 1 and 2). The ~104-m-thick sill has vertical columnar joints that extend upward and downward 5–10 m from its lower and upper margins (Figs. 4B and 9B). We considered the possibility that this deposit represents a welded tuff, which could explain its remarkable concordance, but in thin section, vitroclastic textures are absent, and the hornblende phenocrysts coarsen toward the center of the body (from 0.5 to 2 mm), consistent with an origin as a sill. We believe that the sill owes its remarkable concordance to the fact that it exploited a weak layer in the Relief Peak Formation debris flow deposits, i.e., a rhyolite ash-fall deposit (sample JHSP3;

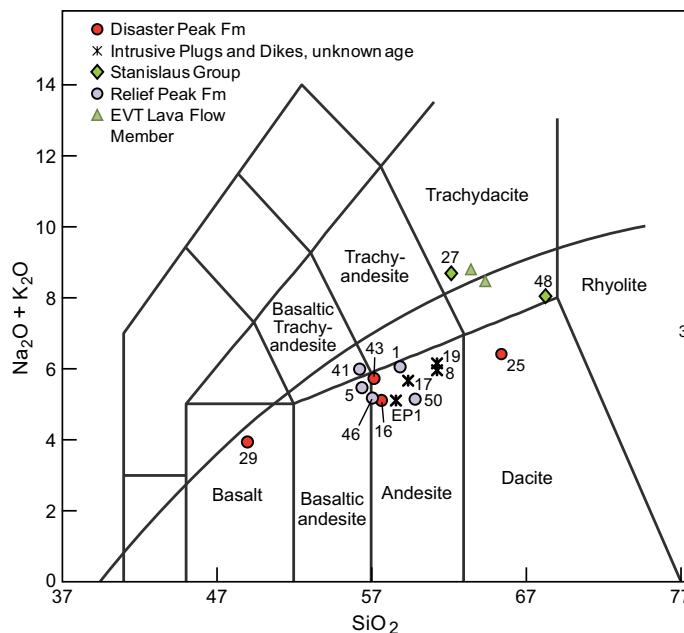


Figure 7. Alkali-silica plot (after Le Bas et al., 1986) showing compositions of 17 rock samples from the area mapped in Figure 2 (samples plotted there); geochemical data and global positioning system locations are given in Table 2. Fm—formation; Mem—member; EVT—Eureka Valley Tuff. EVT Lava Flow Member trachydacite (Tsel) from Koerner et al. (2009) (see sample numbers AAK-08-825 and AAK-08-830 in Table 2), shown for comparison with sample 27 trachydacite. The Lava Flow Member lies between EVT Tollhouse Flat Member and EVT By Day Member along the western margin of the Sierra Crest graben (also see Busby et al., 2013a). Sample 27 trachydacite (at the north end of Fig. 2A) is generalized as Stanislaus Group, because it may be either Lava Flow Member (i.e., within EVT), or it may be equivalent to the newly recognized Basal Lava Member of Busby et al. (2013a), which is between TML and EVT in age (see discussion in text).

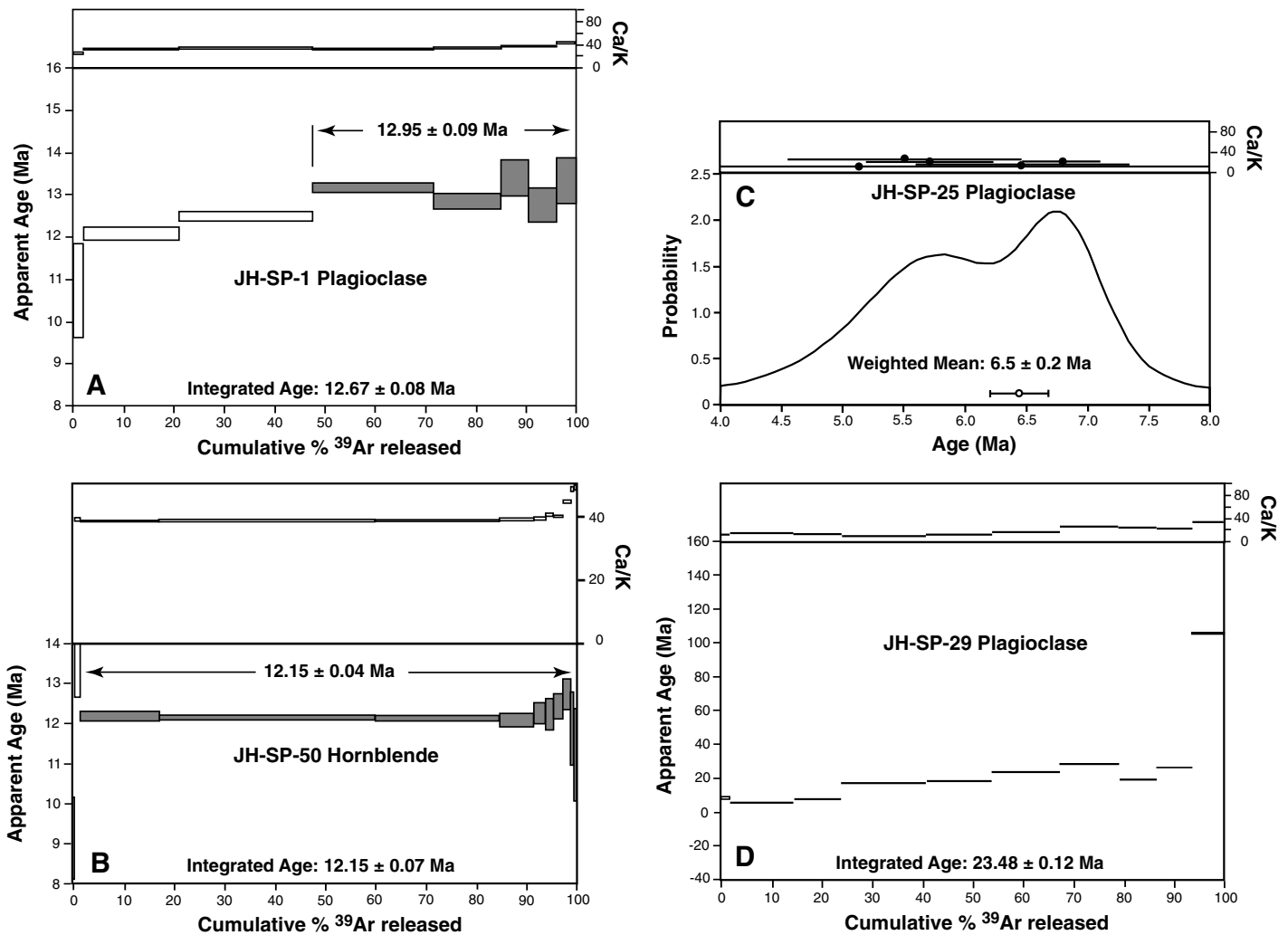


Figure 8. New $^{40}\text{Ar}/^{39}\text{Ar}$ age data for samples from the Sonora Pass range front, arranged from oldest to youngest. Dating methods are summarized in Appendix 1. Sample locations are plotted on the geologic map (Fig. 2); modal analyses are presented in Figure 6 and Table 2, and geochemistry is presented in Figure 7 and Table 1. (A) Two-pyroxene olivine andesite within the Stanislaus Group section in the Lost Cannon fault block (sample SP-1), mapped as Ta (Tertiary andesite) in Figure 2A. This was initially mapped as an intrusion (Tia; Hagan 2010), but the plagioclase $^{40}\text{Ar}/^{39}\text{Ar}$ plateau age of 12.95 ± 0.09 Ma is too old for Stanislaus Group, unless it is a younger intrusion with xenocrystic plagioclase. If so, the plateau age may be meaningless and the age of the andesite may be indicated by the initial low-temperature steps in the age spectrum (i.e., younger than 12 Ma). Based on its age and on other features (see text), we reinterpret this body to be a slide block, rather than an intrusion. (B) Hornblende andesite sill within Relief Peak Formation in the Grouse Meadows block (sample SP-50, map unit Trpas; Fig. 2). We include this sill in the Relief Peak Formation because of its age (12.15 ± 0.04 Ma, on hornblende). An intrusive rather than extrusive origin is indicated by the very low aspect ratio of the sills (too low for an andesite lava flow), the lack of flow breccia, and the presence of columnar joints along the upper and lower contacts where it cooled against the Relief Peak Formation (Fig. 4B). (C) Plagioclase dacite sill of Wells Peak area (sample SP-25), mapped as Tdpds (Disaster Peak dacite sill; Fig. 2). This sill is in the Chango Lake fault block (Fig. 2), and was previously mapped as a dacite lava flow (Hagan, 2010), but its age (6.5 ± 0.2 Ma on five youngest plagioclase crystals) is too young for it to be a lava flow beneath the Table Mountain Latite (TML). We here reinterpret it as a sill based on its age, and also based on geologic relations described in the text (see Wells Peak Section discussion). (D) Two-pyroxene olivine basalt of Wells Peak area, mapped as Tdpib (Disaster Peak basalt intrusion, sample SP-20; Fig. 2). This intrusion cuts the TML, and passes upward into unconsolidated vent deposits (see Figs. 4E, 4F), so it is presumably postglacial. However, our attempt to determine the age of this intrusion using plagioclase phenocrysts was unsuccessful, because the analyzed phenocrysts are probably xenocrysts (integrated age 23.48 ± 0.12 Ma).

Sierra Nevada range front–Walker Lane faulting in the Ancestral Cascades arc

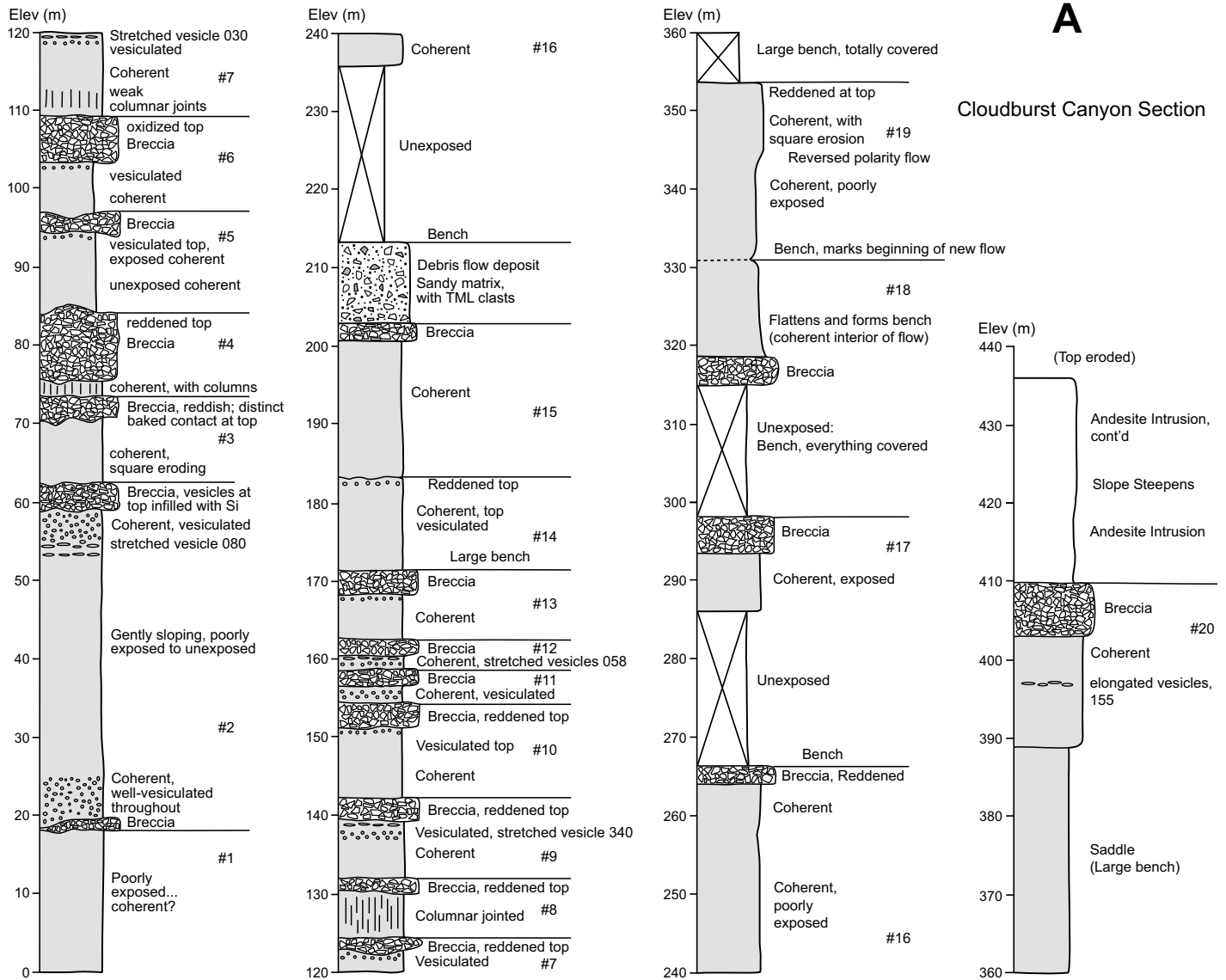


Figure 9 (on this and following page). (A) Measured section through the Table Mountain Latite (TML), along Cloudburst Creek in the Chango Lake fault block (location given in Fig. 2). Paleomagnetic data are available for three of these flows; they are normal polarity and thus not distinctive for correlation purposes (C. Pluhar, 2012, written commun.). Elev—elevation.

Figs. 6 and 7; Tables 1 and 2). Silicic ash-fall deposits are otherwise absent in the Relief Peak Formation, so we describe the tuff in detail here.

The ash-fall deposit is a thin (<1 m) layer at both the bottom and top of the sill (Fig. 9B). In some places it is baked red, along with the debris flow host, and it grades upward into the overlying debris flow deposits above the sill (Fig. 9B). The ash-fall deposit consists of white pumice lapilli (<2 cm) and lesser small (<1 cm) volcanic rock fragments in a (>80%) matrix of nonwelded bubble-wall shards, with euhedral crystals of plagioclase, embayed quartz, and sanidine (sample 3; Fig. 6). The pumice lapilli are squashed but the glass shards are not sin-

tered, so flattening is probably a diagenetic effect (i.e., they are not fiamme). The thinness and lateral continuity of the deposit along with weak (but disrupted) stratification suggest that it is a fall deposit and not an unwelded ignimbrite. Because the sill follows this pyroclastic layer, we suspect that it was intruded before the tuff was fully lithified.

In situ primary volcanic rocks suitable for dating are absent in the Relief Peak Formation sections described herein, so we sampled the sill to get a minimum age on the formation. The ⁴⁰Ar/³⁹Ar hornblende age of the sill is 12.15 ± 0.04 (Fig. 8B), older than the oldest age known age for high-K volcanic rocks of the Stanislaus

Group (11.55 ± 0.07 Ma plagioclase date on a slide block of latite; Busby et al., 2013b). Consequently, we group this andesite sill with the Relief Peak Formation (Trpas).

The TML section in the Grouse Meadows block appears to be less complete than the Cloudburst Creek section to the west (Fig. 2), and that in turn appears to form a less complete section than the TML to the west at Sonora Pass, where vent deposits are mapped (Fig. 10; Busby et al., 2013a). The TML on Sonora Peak at Sonora Pass contains reverse polarity flows at two stratigraphic levels (Busby et al., 2008a), whereas the Cloudburst Creek section has a reverse polarity flow at only one strati-

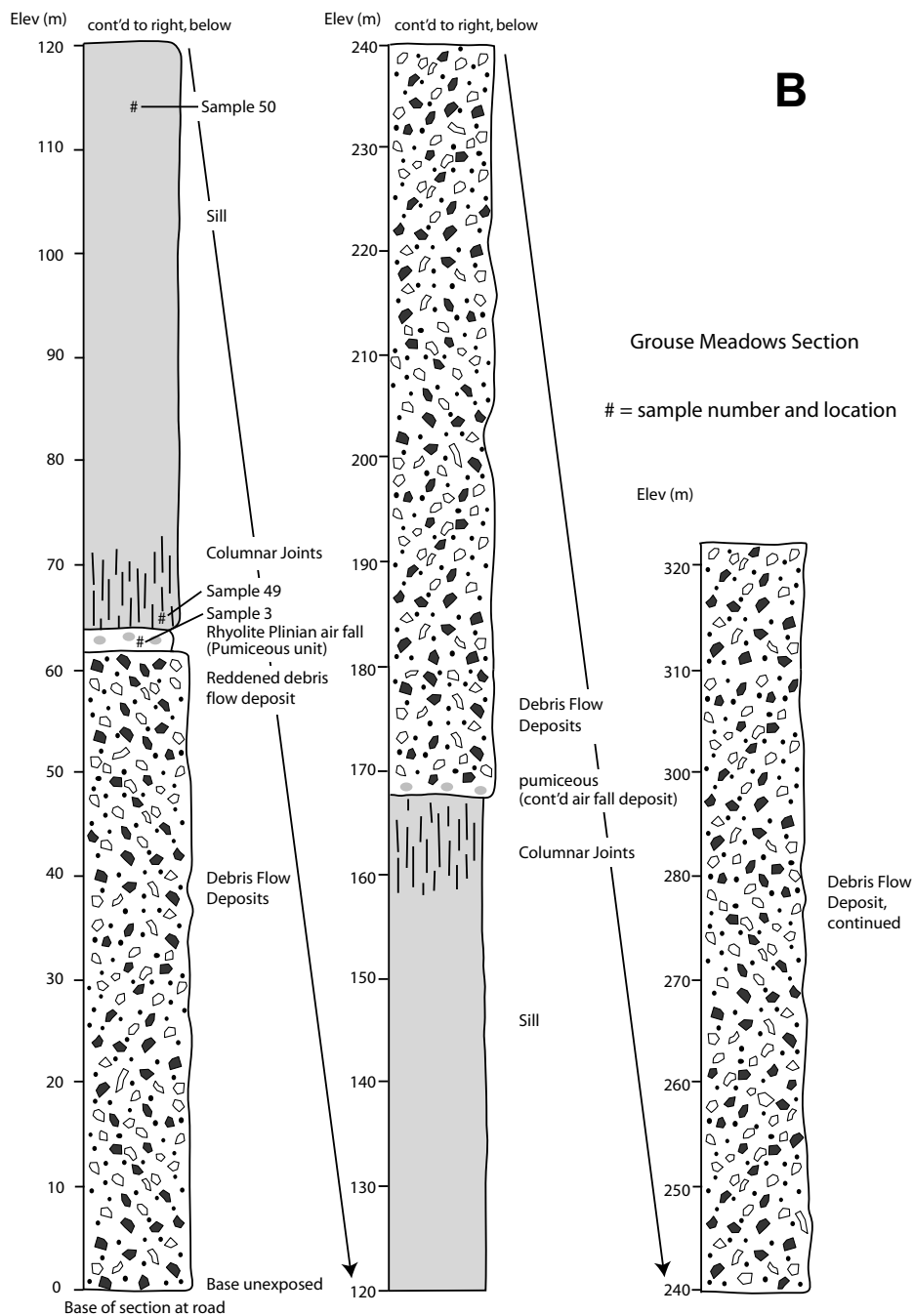


Figure 9 (continued). (B) Measured section through massive debris flow deposits of the Relief Peak Formation in the Grouse Meadows fault block, showing the ~100-m-thick andesite sill that intrudes it (map unit Trpas; see Fig. 2). Sample 50 from the sill is andesite (Fig. 7). Sample 3 is from the sole rhyolite Plinian fall deposit within the Relief Peak Formation (also plotted in Fig. 7).

graphic level, and the Grouse Meadows lava flows all have normal polarity (Busby et al., 2008a; Pluhar et al., 2009). Local hiatuses and/or erosion within the TML section in the Grouse Meadows block may be indicated by fluvial sandstones at three stratigraphic levels

(see fig. 10B of Busby et al., 2008b), one of which is thick enough (~5 m) to map along much of the length of the TML in the Grouse Meadows half-graben (Tstmf; Fig. 2).

The EVT Tollhouse Flat member is not preserved between TML and the EVT By-Day

Member in the Grouse Meadows fault block, although it is present in the block to the west, where the TML is much thicker (Busby and Wagner, 2006; Busby et al., 2008a; Pluhar et al., 2009).

Grouse Meadows Fault

The Grouse Meadows fault mainly is in a valley with spring-fed vegetation along it (Fig. 5C), and drops the TML and EVT By-Day Member down against the Relief Peak Formation (Figs. 2 and 3A). The top of the TML is dropped down to the west with a vertical displacement of ~760 m, and the vertical displacement on the base is even greater, estimated as ~1100 m. The fault is exposed at its north end (Fig. 2), where it drops the Relief Peak Formation down against highly brecciated granitic rock; pieces of this granite that litter the ground have planar surfaces with slickenlines, but no in situ fault surfaces have been identified. The mapped trace of the fault strikes N40°E, dips 60°E, and is curved, so we infer that it is concave upward at depth (Figs. 2 and 3A). The Grouse Meadows fault appears to die out northeastward, where the TML does not appear to be tilted, and does not appear to be downdropped, because its base is ~122 m higher (Fig. 2); however, there is not enough of it preserved there to prove the former, and the latter could be due to paleotopographic effects (on unconformity 3; Fig. 2C).

Stratigraphy of the Lost Cannon Fault Block

The Lost Cannon fault block is the longest fault block in the study area (see Fig. 2B). Like the Chango Lake fault to the west, it drops Cenozoic volcanic rocks down to the east against granitic basement. These strata are described in two areas: the Mean Peak section in the south, and the Lost Cannon Creek section in the north (Fig. 2A).

Mean Peak Section and Faults Therein

The section at Mean Peak is similar to that at Grouse Meadows, with several key differences. The Relief Peak Formation debris flow deposit (Trpdf; Fig. 2) does not have Valley Springs Formation ignimbrite slide blocks or slide blocks of Relief Peak Formation andesite block-and-ash-flow tuff, although it contains a minor lens of in situ andesite block-and-ash-flow tuff (not mapped separately; Fig. 2). The TML lava flows thicken dramatically southward within the fault block, from 190 m in the north (similar to the thickness in the Grouse Meadows block) to 390 m in the south (Fig. 2). The thickness of the mappable fluvial sandstone bed (Tstmf) within

Sierra Nevada range front—Walker Lane faulting in the Ancestral Cascades arc

the TML also increases southward, where it parallels the Lost Cannon fault (from 0 to 10 m), and then thickens much more to the west toward the fault (from 10 m to >60 m; Figs. 2 and 3A). Morainal covers prevent determining whether the lower part of the TML thickens westward toward the fault, but the part above the sandstone appears to thicken toward the fault (Figs. 2 and 3A). Where the sandstone is thickest (against the fault), it forms a fining-upward sequence of beds, with basal medium-bedded, moderately well sorted, pebble conglomerate passing upward into well-sorted coarse-grained sandstone and lesser pebble conglomerate, which passes upward into well-sorted, thin-bedded, medium- to fine-grained sandstone (all with planar laminations and trough cross-laminations).

The Tollhouse Flat and overlying By-Day Members of the EVT form extensive dip slopes of resistant welded ignimbrite on top of the TML, dipping 27°NW toward the Lost Cannon fault; however, where the ignimbrites can be viewed in cross section along the Mean Peak ridge crest, they are only ~10 m thick. The Tollhouse Flat Member fills a channel cut into TML at the north end of the ridge, and the overlying By-Day Member fills a channel cut into it and TML. A smaller channel filled with the Tollhouse Flat Member forms a lens beneath the By-Day Member just east of Mean Peak (Tset; Fig. 2), where it is nonwelded.

The contact between the TML and EVT at this locality is of interest because an andesite (sample SP-1; Figs. 6 and 7) is within the Stanislaus Group section here. This andesite was first mapped as an intrusion (Tia; Hagan 2010) because its contacts with the TML, which largely enclose it, are discordant to TML lava flow layering; also, the andesite differs from the TML by being much lighter in color and containing lower K₂O. However, the upper contact of the andesite passes from coherent through brecciated andesite into what appears to be a depositional contact with overlying By-Day Member. A new ⁴⁰Ar/³⁹Ar plagioclase age of 12.95 ± 0.09 Ma on this andesite (Fig. 8B) shows that it is too old to represent an intrusion cutting the Stanislaus Group, unless the plagioclase is all xenocrystic. More likely, the dated andesite represents a slide block derived from Relief Peak Formation; two more lenses of andesite that are along strike of this body (Fig. 2) may represent additional slide blocks. This andesite is somewhat unusual mineralogically because although it has a silica content of 58.8%, it contains 3% olivine phenocrysts (JHSP-1; Figs. 6 and 7; Tables 1 and 2).

Two vertical faults, restricted to the Mean Peak block, strike perpendicular to the Lost Cannon fault in its hanging wall (~318° and

TABLE 1. MODAL ANALYSIS DATA FOR THE SAMPLES SHOWN IN GRAPH FORM IN FIGURE 6

Unit	Oxide	Plagioclase	Olivine	Cpx	Opx	Hornblende	Biotite	Kspar	Quartz	Sphene	Lithic clasts	Pumice clasts	Glass	Altered	Groundmass	Rims	Sum
Basalt intrusion of Wells Peak (Tdpib; 29)	0	13.7	11.8	7.6	2	0	0	0	0	0	0	0	0	3.1	61.8	0	100
Andesite intrusion north of Antelope Peak (Tai; JHEP-1)	0.9	4	0	0	0	0	0	0	0	0.1	0	0	0.3	0	94.7	0	100
Northern andesite intrusion of Lost Cannon Creek (Tdpai; 16)	3.2	0.3	0	7	0.8	0	0	0	0	0	0	0	0	3.4	81.5	3.8	100
Andesite sill of Grouse Meadows (Tias; 50)	1	2.3	0	0	0	17.7	0	0	0	0	0	0	0	11.3	67.7	0	100
North-central andesite intrusion of Lost Cannon Creek (Tai; 19)	4.2	11.3	0	0	0	8.5	0	0	0	0	0	0	0	1.3	74.7	0	100
South-central andesite intrusion of Lost Cannon Creek (Tai; 17)	3.7	17.4	0	0	0	17.7	0.2	0	0	0	0	0	0	9.7	51.3	0	100
Andesite intrusion of Mean Peak (Tdpai; 01)	3.5	26.4	2.9	6.4	0.7	0	0	0	0	0	0	0	0	3	57.1	0	100
EVT: By-Day Member (Tseb; 48)	0.8	11.2	0	2	0.3	0	0	0	0	0	11.4	18.7	52.5	3.1	0	0	100
EVT: Tollhouse Flat Member (Tset; 31)	1.4	7.8	0	1.5	0	0	2.2	0	0	0	8.8	41.5	35.4	1.4	0	0	100
Andesite block from homogeneous debris flow deposit (Trpdf; 46)	2	26.2	0	5.2	5.2	0	0	0	0	0	0	0	13.7	0	47.7	0	100
Block-and-ash flow within debris flow (within Trpdf; 05)	3.7	18.3	0	4	0	4.7	0	0	0	0	0	0	0	9	60.3	0	100
Dacite sill at Wells Peak (Tdpds; 25)	1.8	9.6	0	0	0	0	0	14	2.8	0	0	0	3.5	0	68.3	0	100
Phyolite ash fall (within Trpdf; 03)	0.5	8.1	0	0	0	0	0	3.8	4.8	0	3.8	7.5	71.5	0	0	0	100

Note: Numbers for each component (e.g., oxide, plagioclase, groundmass) are given in percentage of total rock (= sum of 100%); percentages of components for each sample are continued onto second line. Abbreviations and numbers in parentheses refer to map unit symbol (Fig. 2C) and sample number, in that order. All samples are plotted on the geologic map (Figs. 2A and 2B) with the prefix SP (for Sonora Pass), except for the northernmost one, which is identified here as JHEP-1 and plotted as such on the map. GPS locations given in Table 2. GPS—geographic positioning system; EVT—Eureka Valley Tuff; Cpx—clinopyroxene; Opx—orthopyroxene; Kspar—K-feldspar.

TABLE 2. GEOCHEMICAL DATA AND GPS LOCATIONS FOR THE SAMPLES PLOTTED ON THE ALKALI-SILICA DIAGRAM (FIGURE 7)

Unit	Sample number	SiO ₂	TiO ₂	Al ₂ O ₃	Fe ₂ O ₃	MnO	MgO	CaO	Na ₂ O	K ₂ O	P ₂ O ₅	Cr (ppm)	Sum	Geochemistry	Latitude (°N)	Longitude (°W)
Tdpib	JHSP-29	48.95	1.91	15.71	9.79	0.12	9.16	10.2	2.58	1.36	0.475	417.1	100.32	basalt	38.416	119.589
Tdpla	JHSP-16	57.62	0.965	18.15	7.34	0.07	4.08	6.23	3.38	1.74	0.258	0	99.828	andesite	38.487	119.509
Tdpla	JHSP-43	57.15	1.07	17.45	7.11	0.16	3.65	7.38	3.28	2.45	0.404	170.4	100.12	andesite	38.357	119.571
Tia	JHSP-8	61.23	0.8	17.97	5.36	0.06	2.71	5.62	3.68	2.27	0.291	13.5	99.992	andesite	38.434	119.528
Tia	JHSP-17	59.37	0.92	17.87	6.04	0.05	2.99	6.69	3.8	1.86	0.333	0	99.923	andesite	38.463	119.521
Tia	JHSP-19	61.245	0.675	18.38	5.095	0.06	1.99	5.67	3.66	2.48	0.336	0	99.581	andesite	38.469	119.509
Tia	JHEP-1	58.62	0.67	19.34	7.22	0.11	2.05	6.21	3.16	1.98	0.417	3.2	99.777	andesite	38.511	119.566
Tseil	JHSP-27	62.19	1.4	16.77	5.65	0.05	1.49	3.31	3.36	5.32	0.495	1.3	100.03	trachydacite	38.450	119.575
Tseb	JHSP-48	68.23	0.585	15.8	3.98	0.04	0.84	2.36	2.9	5.13	0.135	1.05	99.994	trachydacite	38.450	119.527
Tsia	JHSP-01	58.82	0.92	17.75	6.69	0.07	3.42	6.08	3.48	2.58	0.331	0	100.14	andesite	38.398	119.522
Trpdf*	JHSP-46	57.005	0.915	17.98	7.43	0.1	3.975	7.46	2.915	2.25	0.314	0	100.33	andesite	38.460	119.523
Tias	JHSP-50	59.8	0.82	17.3	5.97	0.06	3.87	6.64	3.35	1.79	0.218	0	99.818	andesite	38.393	119.489
Trpdf†	JHSP-3	77.66	0.18	13.48	1.37	0.02	0.76	0.62	1.44	5.29	0.02	6.2	100.84	rhyolite	38.393	119.488
Tdpds	JHSP-25	65.285	0.485	18.955	3.845	0.01	0.275	4.53	3.67	2.7	0.268	5.05	100.01	dacite	38.395	119.593
Trpdf*	JHSP-5	56.36	1.21	18.44	7.58	0.06	3.22	7.26	3.13	2.34	0.419	9	100.02	basaltic andesite	38.393	119.490
Tstml?	JHSP-41	56.21	1.12	17.52	7.33	0.1	3.7	7.72	3.9	2.08	0.389	0	100.07	trachybasaltic andesite	38.335	119.662
Tseif‡	AAK-08-825	63.46	1.12	17.1	4.93	0.04	1.24	2.94	3.46	5.34	0.37	—	100	trachydacite	38.374	119.764
Tseif‡	AAK-08-830	64.36	1.1	17.2	4.73	0.05	1.06	2.7	3.18	5.3	0.37	—	100.05	trachydacite	38.373	119.752

Note: "Unit" refers to map units shown in Figure 2C; sample numbers are plotted on the geologic map (Figs. 2A and 2B) with the prefix SP (for Sonora Pass) except for the northernmost one, which is identified here as JHEP-1 and plotted as such on the maps. All values (e.g., SiO₂) are given in percent except Cr (in ppm).

*Sample of block-and-ash flow tuff within debris flow deposit.

†Sample of ash-fall tuff within debris flow deposit.

‡Data previously published in Koerner et al. (2009).

~335°). Along each fault, all contacts between mapped units are offset by the same amount. It is not clear whether these are dextral strike-slip faults, or normal faults with down to the northeast displacement, or a combination (Figs. 2 and 3A). The displacement across the north fault is estimated as ~100 m laterally and 15 m vertically, and on the south fault is ~75 m laterally and 18 m vertically.

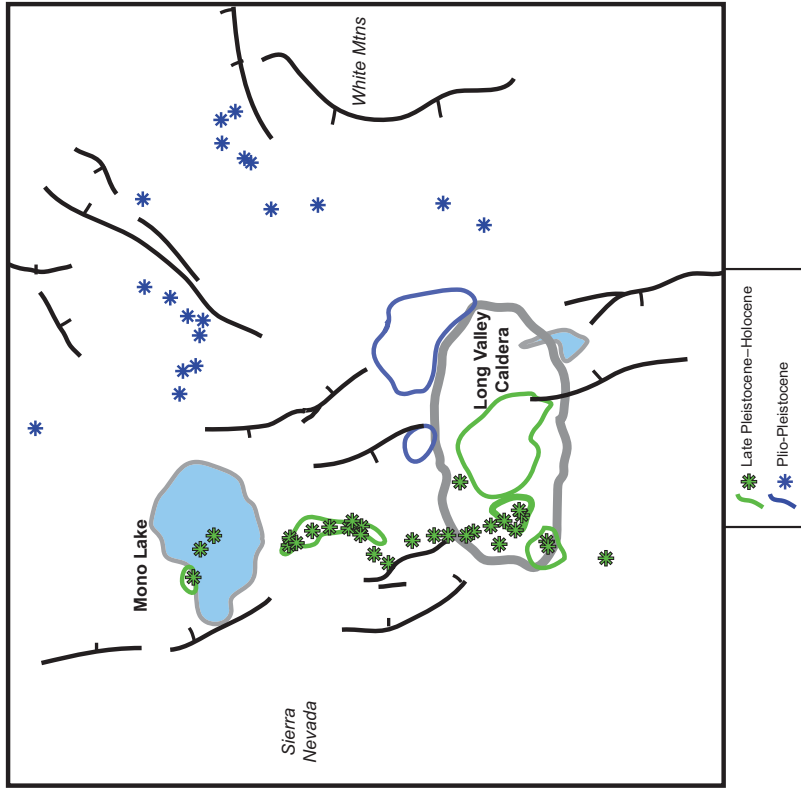
Lost Cannon Creek Section

The Lost Cannon Creek section (Fig. 3D) differs from the Grouse Meadows and Mean Peak sections (Fig. 3A) in that it has 245–365 m of in situ Valley Springs Formation at the base (Tvs; Fig. 9). The contact between Valley Springs Formation and the granitic basement was mapped as a fault by Slemmons (1953), but it is depositional, with ignimbrite welding foliations parallel to the contact, and a total lack of brecciation or shear zones along the contact. Welding compaction in the Valley Springs Formation ignimbrites dips ~40° westward or northwestward toward the Lost Cannon fault (Fig. 2). A deep erosional unconformity (unconformity 2), with several tens of meters of relief, separates the Valley Springs Formation from the overlying Relief Peak Formation, and this surface is overlain by an ~1–3-m-thick boulder conglomerate bed at the base of the Relief Peak Formation, which also dips ~40° westward. The conglomerate is well sorted, with rounded granitic and andesitic boulders and cobbles, and is clearly of fluvial origin (see photo in fig. 6D of Busby and Putirka, 2009). The presence of in situ Valley Springs Formation and overlying fluvial boulder conglomerate indicates deposition in a paleochannel. However, the overlying Relief Peak Formation debris flow deposits contain abundant Valley Springs Formation megablocks as much as 40 m long (Trpdfi), so accommodation of that part of the section was probably at least in part provided by syndepositional normal faulting. Andesite clasts in the Relief Peak Formation debris flow deposits here appear largely monolithic, and are dark colored; they have plagioclase and two pyroxenes, and the chemistry of one sample plots on the boundary between andesite and basaltic andesite (sample SP46; Figs. 6 and 7; Tables 1 and 2).

Bedding dips are considerably shallower in strata of the Stanislaus Group than they are in the underlying Valley Springs and Relief Peak Formations (Figs. 2 and 3D); this indicates tilting toward the Lost Cannon fault during deposition. Erosional remnants of TML and the By-Day Member of the EVT along the ridge crest dip 10°–20° toward the Lost Cannon fault. The erosional remnants of TML include a southern remnant with three flows, one with large, sieve-

Sierra Nevada range front–Walker Lane faulting in the Ancestral Cascades arc

B Long Valley Caldera
Southern Sierra Nevada



A Ebbetts Pass–Sonora Pass
Central Sierra Nevada

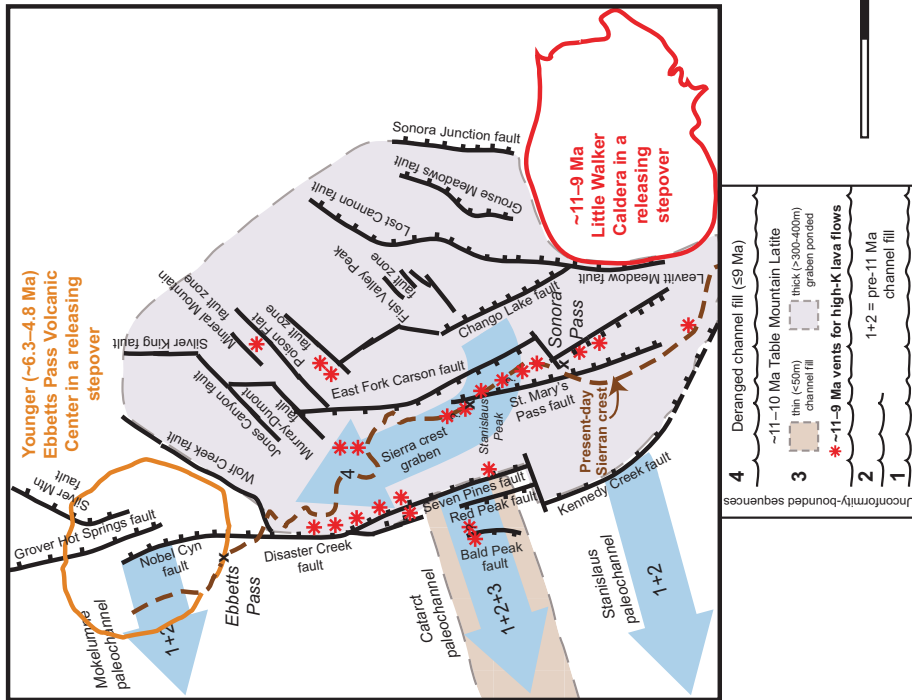


Figure 10. Synvolcanic faults and vents for the ca. 11.5–9 Ma Sierra Crest graben–Little Walker volcanic center (left), compared with transensional faults of Long Valley volcanic field (right) at the same scale (Long Valley modified from Bursik, 2009). (A) Position of the range-front faults at Sonora Pass (this study), relative to the Sierra Crest graben-vent system to the west and north (Busby et al., 2013a), and the Little Walker caldera to the south. This figure shows all the vent areas we have mapped for the Stanislaus Group high-K volcanic rocks. Effusive rocks erupted from an area covering at least 250 km², and explosive rocks were mainly erupted from the Little Walker caldera (see text). The lavender-gray colored area shows the region of ponding of trachyandesite and trachyandesite flood lavas of the Table Mountain Latite (TML), as well as Eureka Valley Tuff Lava Flow Member lavas (which include trachydacite as well as trachyandesite lava). Vents (red stars) are mainly fault-controlled fissures, with minor point sources. They are within the north-northwest–south-southeast Sierra Crest graben, in north-northwest–south-southeast half-grabens that affected the Cataract paleochannel on the west (Bald Peak–Red Peak area), and in northeast-southwest transfer zone faults and basins along the northeast boundary of the graben. Note the position of the modern Sierra Nevada crest; most fault reactivation since 9 Ma has occurred to the east of the crest, on the modern range front. No high-K vents are associated with range-front faults along the southeast side of the Sierra Crest vent-graben system, but as shown in this study, half of the slip on these faults occurred before or during deposition of the TML. This system of faults steps right in a releasing stepover, like that controlling the position of the Long Valley caldera. (B) Releasing stepover controlling the position of the Long Valley caldera (modified from Bursik, 2009; also see Riley et al., 2012); the culminating silicic explosive eruptions at the Little Walker caldera (Eureka Valley Tuff) formed under a similar strain regime, but in the upper plate of a subduction zone, rather than in a rift setting, which prevails at Long Valley.

textured plagioclase phenocrysts, and a northern remnant entirely composed of the flow with the large sieve-textured plagioclase phenocrysts. A thin (2–3 m) erosional remnant of By-Day Member forms a very small exposure (40 m × 15 m), but the surrounding area is littered with float, where the tops of the underlying debris flow outcrops are reddened through baking, indicating that the EVT was originally more extensive. The outcrop is a black vitrophyre with abundant 6-cm-long fiamme and pebble-sized accidental rock fragments; trace amounts of biotite phenocrysts are visible only in thin section in trace amounts (sample 48; Fig. 6), in contrast to Tollhouse Flat Member, which has obvious biotite (sample 31; Fig. 6, from the north end of the Lost Cannon block). In thin section, plagioclase is grown around clinopyroxene crystals. A whole-rock analysis (not on pumice) plots in the trachydacite field (sample 48; Fig. 7).

A series of andesite plugs intrudes rocks of the hanging-wall section at Lost Cannon Creek; these are generally absent from the granitic footwall block (Fig. 2). This may be because the intrusions followed the fault through the basement until they reached less competent basin fill at shallow levels, and then moved up through it. These andesites are mainly mapped as intrusions of unknown age (Tia, samples SP8, SP17, SP19) because most of them cut the oldest andesitic rocks (Relief Peak Formation), but the northernmost one cuts Stanislaus Group rocks and is thus mapped as Disaster Peak Formation (Tdpia, sample SP16; Fig. 2). All of these samples plot in the andesite field in Figure 7 (and see Table 2). The andesite intrusions of unknown age are plagioclase and hornblende rich (see modal analysis sample SP17; Fig. 6; Table 1), whereas the Disaster Peak andesite intrusion contains clinopyroxene and minor plagioclase and orthopyroxene (SP16; Fig. 6; Table 1). Only one andesite intrusion crops out in the footwall, where it intrudes the Relief Peak Formation north of Antelope Peak (Fig. 2); this intrusion is phenocryst poor, with 4% plagioclase and 0.1% sphene (sample JHEP-1; Fig. 6; Table 1), and thus is not correlative with any of the hanging-wall intrusions.

Lost Cannon Fault

The Lost Cannon fault (Fig. 2) is more than 18 km long and drops Tertiary volcanic rocks down on the east against granitic basement on the west (Figs. 2, 3A, and 3D). The fault trace is deflected across topography and dips ~60°E. We infer that it is concave up at depth by Mean Peak (Fig. 3A) but it may be more planar at depth beneath Lost Cannon Creek (Fig. 3D) because its trace is more linear and strikes 020°,

although strata are clearly rotated toward the fault (Figs. 2 and 3D). South of Mean Peak, the fault is largely buried beneath Quaternary deposits and merges with the Leavitt Meadow fault at its southern extent.

Along Lost Cannon Creek, welding compaction in the Valley Springs Formation ignimbrites and stratification in the Relief Peak Formation dip ~40°–45° toward the fault (Figs. 2 and 3D); although debris flows can have primary dips, the consistent welding compaction fabric in the Valley Springs Formation is a good indicator of paleohorizontal. That Valley Springs and Relief Peak Formation rocks are absent from the footwall of the Lost Cannon fault requires at least 1250 m (Fig. 3D) displacement across the fault. In contrast, the overlying TML lava flows dip only ~10° toward the Lost Cannon fault. The discordance can be explained by arguing that the TML lavas draped a >30° dipping erosional surface cut into the older strata. However, TML flows do not dip more than ~1°–2° in the unfaulted Sierran block to the west. In addition, these lavas must have had low viscosities to allow them to flow so far down the paleochannels (see fig. 1 of Busby *et al.*, 2013a); this precludes their having had significant primary dips. These characteristics indicate that the TML primary dips were very low. Consequently, the TML lava flows are offset 505 m by normal displacement along the Lost Cannon fault, which indicates that nearly half of the displacement on this section of the Lost Cannon fault occurred before the emplacement of the TML.

At Mean Peak, the TML lava flows are offset across the Lost Cannon fault by at least 762 m, as measured from the projected base of the flows to the elevation of the granitic basement in the footwall directly to the west (Fig. 3A). However, if the elevation of the contact between granitic basement and TML only ~1 km to the north of the line of section is used (at 11,000 ft [~3353 m] on Lost Cannon Peak; Fig. 2), the estimated offset of the base of the TML is >1250 m. If so, the offset of TML here is as great as the offset of the base of the Cenozoic section (Valley Springs Formation) farther north in Lost Cannon Creek, which suggests that offset along the Lost Cannon fault increases from north to south.

Leavitt Meadow Fault

The Chango Lake fault and the Lost Cannon fault merge to the south, becoming the Leavitt Meadow fault, which Slemmons (1953) estimated to have a throw of >610 m down to the east. However, the height of the well-developed escarpment in the granitic basement south of Highway 108 (red line, Fig. 2B) implies >730 m. We cannot estimate the offset of the base of the

volcanic section across the fault. Although the base of the volcanic section is not exposed on the hanging wall, assuming the rocks in the hanging wall are strata (and not intrusions), a minimum vertical displacement of 485 m is required; this minimum is unlikely because of the height of the modern escarpment. However, rocks exposed in this area may include intrusions (Priest, 1979), and mapping and analytical work are needed.

We concur with Slemmons's (1953) inference that the Leavitt Meadow fault continues at least as far south as Mount Emma, which is in the Little Walker caldera (Priest, 1979), the source of the EVT (King *et al.*, 2007) (Fig. 2). The TML is not exposed in the hanging wall of the Leavitt Meadow fault, so the timing of displacement along the fault relative to deposition of the TML is indeterminate. However, because the Leavitt Meadow fault extends northward into the Lost Cannon fault, which was active contemporaneously with eruption of the TML, it seems likely that the Leavitt Meadow fault was also active contemporaneously with eruption of the TML. The southern end of the Leavitt Meadow fault has not, to our knowledge, been mapped.

We infer that the TML underlies the Little Walker caldera at depth, as the TML also occurs south of the caldera, where it flowed southwestward down a paleochannel that is nearly 20 km south of the area mapped in Figure 2 (see fig. 1 of Busby *et al.*, 2013a). If so, offset of the TML along the Leavitt Meadow fault is much greater than that shown by the geomorphic scarp.

CONCLUSIONS

Prevolcanic to synvolcanic offset is more difficult to demonstrate than postvolcanic offset on faults in the Sierra Nevada range front at Sonora Pass, and has not been previously recognized. Separating the effects of paleorelief from those of syndepositional faulting requires detailed mapping. Our mapping shows that the TML was ponded to thicknesses of as much as 400 m in actively subsiding eastern range-front half-grabens. This contrasts markedly with the TML just east of the range front, directly across Highway 395 (see Fig. 2B), where the TML is <150 m thick (commonly much thinner), and consists of only 1–5 flows (King *et al.*, 2007; Pluhar *et al.*, 2009). The dramatically enhanced thickness of the TML west of Highway 395 is attributable to synvolcanic extension in what are now the range crest (Busby *et al.*, 2013a) and range-front areas (this study).

Faults in the Sierra Nevada range front at Sonora Pass generally trend approximately north-northwest to north-south, exhibit down to the east slip, displace Miocene volcanic and

volcaniclastic rocks against Mesozoic basement, and exhibit increasing throw southward, toward the Little Walker caldera. Pre-TML displacement on the Chango Lake fault cannot be determined, due to the absence of pre-TML strata on the footwall, but we infer that this absence reflects uplift of a horst block between the Chango Lake fault and the East Fork Carson fault. The horst block provided a source for the voluminous debris avalanche deposits to the west in the Sierra Crest graben (Busby et al., 2013a). The presence of the 110-m-thick dacite sill of Disaster Peak on the hanging wall of the Chango Lake fault at Wells Peak suggests that ascending magma exploited the fault. Vertical displacement of the base of the TML increases southward on the Chango lake fault, from 182 m to 550 m. The pre-TML displacement on the Lost Cannon fault is estimated as 60% of its total displacement (745 m before versus 505 m after). This fault also displays increasing displacement southward, from 505 to 1250 m, or the base of the TML. The morphological expression of the Leavitt Meadow fault further south indicates a minimum vertical displacement of 730 m, but the inferred presence of the TML beneath the Little Walker caldera suggests much greater displacement. The Grouse Meadows fault offsets the base of the TML substantially more than its top (1100 versus 760 m), indicating slip during eruption of the TML, but we also infer that the 600-m-thick Relief Peak Formation below the TML was deposited catastrophically during subsidence in the half-graben just before the TML was erupted. Because faults in the study area are fairly steep, the amount of extension is probably low (~10%); however, that is a minimum estimate, because the post-TML, pre-EVT throw on the Leavitt Meadow fault is not known.

In addition to the north-northwest to north-south normal faults described herein, the northern end of the study area contains a northeast sinistral-oblique normal fault zone (Fish Valley Peak fault zone) that transfers extension from the Chango Lake fault to the Lost Cannon fault. This fault zone appears to be an oblique down to the northwest sinistral synvolcanic fault zone that was later rotated ~30° by down to the east extension on the north-south Fish Canyon fault. This transfer fault zone forms the southern boundary of a 25-km-wide northeast fault transfer zone that strikes obliquely down the modern Sierra Nevada range front between the study area and Ebbetts Pass (Fig. 10; for detailed maps, see Busby et al. 2013a). The 25-km-wide transfer zone forms the northeast boundary of the Sierra Crest graben vent system (Fig. 10; Busby et al., 2013a). The major northeast transfer zone is significant because north-east to east-northeast sinistral-oblique normal

fault zones form an important component of the transtensional Walker Lane belt, particularly in the central Walker Lane (which contains the study area), and are not a prominent feature of the Basin and Range extensional province (for further discussion, see Busby, 2013b).

It was previously inferred that the Sierra Nevada range-front faults at Sonora Pass form a system that steps right (northeastward), and it was suggested that the Little Walker caldera formed in a releasing stepover (Putirka and Busby, 2007; Busby et al., 2008a, 2010); however, most of the faults of the range front had not yet been mapped in detail when those inferences were made. We have provided detailed documentation of range-front fault slip histories, showing that at least half of the slip on the range-front faults occurred before and during eruption of the TML, prior to eruption of the EVT and development of its source caldera; we also show that throw on the faults increases toward the caldera. This supports our interpretation that the range-front faults controlled the siting of the caldera. At the time of our earlier papers (Putirka and Busby, 2007; Busby et al., 2008a), we did not realize that the right-stepping fault system on the range front at Sonora Pass forms only a part of the larger structural stepover shown in Figure 10. The scale of this structural stepover was not previously appreciated because the Sierra crest graben-vent system and the 30-km-wide transfer zone that emanates from its northeast boundary had not been mapped (for details, see Busby et al., 2013a). We conclude that the Sierra Crest graben-vent system and the Little Walker caldera together formed a very large transtensional volcanic field that formed in the heart of the Ancestral Cascades arc ca. 12 Ma. This very large transtensional volcanic field records the birth of a new transtensional plate boundary (Busby et al., 2010, 2013b).

ACKNOWLEDGMENTS

This research was supported by National Science Foundation grants EAR-01252 (to Busby, Gans, and Skilling), EAR-0711276 (to Putirka and Busby), and EAR-0711181 (to Busby), as well as U.S. Geological Survey EDMAP program awards 06HQA061 and 09HQPA0004 (to Busby) and the University of California–Santa Barbara (UCSB) Academic Senate (award to Busby). Additional support came from the Northern California Geological Society, the American Alpine Club, and UCSB's graduate division (Hagan). Field assistance was provided by Maia Davis, Carolyn Gorny, Chip Hagan, and Senator Kay Hagan. We also thank UCSB summer field camp 2006 for their assistance in mapping the Mean Peak area. We thank David Wagner (California Geological Survey) for encouraging Busby to begin work in the Sierra Nevada, and for his many valuable discussions with us at all stages of the work, especially field discussions. We thank Art Sylvester for serving on Hagan's thesis committee

(even though he is officially retired from UCSB) and helping her a great deal with her thesis writing. Busby thanks Charles Rogers at Rogue City College, for taking her on a long ride in his private plane, so she could take the oblique air photos presented in this paper. We also thank Graham Andrews for preparing the oblique view of part of our map shown in Figure 5B.

We thank Keith Putirka, Chris Pluhar, David John, Jason Saleeby, Chris Henry, George Bergantz, Burt Slemmons, Ed Du Bray, John Platte, Ellen Platzman, and the participants of the 2010 GSA Penrose conference for field discussions, and Putirka for training Hagan in his geochemistry lab and showing her how to plot and interpret the results.

We thank Elizabeth Miller, David John, Ed DuBray, and Joe Colgan for formal reviews of this paper.

APPENDIX 1. ⁴⁰Ar/³⁹Ar DATING METHODS

Samples were prepared and analyzed using standard techniques and interference corrections (described in Renne et al., 2013). Fish Canyon sanidine was used as the standard. Samples were analyzed either by total fusion or incremental heating with a CO₂ laser. Samples JHSP-1 (plagioclase), JHSP-29 (plagioclase), and JHSP-50 (hornblende) were analyzed by incremental heating of multigrained aliquots. Sample JHSP-25 (plagioclase) was analyzed by total fusion of individual crystals. Ages were calculated using the calibration of Renne et al. (2011). Age uncertainties stated in the text do not include contributions from decay constants and the isotopic composition of the standard.

REFERENCES CITED

- Armin, R.A., John, D.A., and Dohrenwend, J.C., 1983, Geologic map of the Freel Peak 15-minute quadrangle, California and Nevada: U.S. Geological Survey Miscellaneous Investigations Report I-1424, scale 1:62,500.
- Armin, R.A., John, D.A., Moore, W.J., and Dohrenwend, J.C., 1984, Geologic map of the Markleeville 15-minute quadrangle, Alpine County, California: U.S. Geological Survey Miscellaneous Investigations Series Map I-1474, scale 1:62,500.
- Bursik, M., 2009, A general model for tectonic control of magmatism: Examples from Long Valley Caldera (USA) and El Chichon (Mexico): *Geofísica Internacional*, v. 48, p. 171–183.
- Busby, C.J., and Wagner, D., 2006, Mapping of Cenozoic volcanic rocks in the central high Sierra: Clues to understanding landscape evolution and range-front faulting: National Association of Geoscience Teachers Guidebook, 60 p.
- Busby, C.J., and Putirka, K., 2009, Miocene evolution of the western edge of the Nevadaplano in the central and northern Sierra Nevada: Paleocanyons, magmatism and structure, *in* Ernst, G., ed., *The rise and fall of the Nevadaplano: International Geology Review*, v. 51, p. 671–701, doi:10.1080/00206810902978265.
- Busby, C.J., Hagan, J.C., Putirka, K., Pluhar, C.J., Gans, P.B., Wagner, D.L., Rood, D.H., DeOreo, S.B., and Skilling, I., 2008a, The ancestral Cascades arc: Cenozoic evolution of the central Sierra Nevada (California) and the birth of the new plate boundary, *in* Wright, J.E., and Shervais, J.W., eds., *Ophiolites, arcs, and batholiths: A tribute to Cliff Hopson: Geological Society of America Special Paper 438*, p. 331–378, doi:10.1130/2008.2438(12).
- Busby, C.J., DeOreo, S.B., Skilling, I., Hagan, J.C., and Gans, P.B., 2008b, Carson Pass–Kirkwood paleocanyon system: Implications for the Tertiary evolution of the Sierra Nevada, California: *Geological Society of America Bulletin*, v. 120, p. 274–299, doi:10.1130/B25849.1.
- Busby, C.J., Hagan, J.C., Koerner, A.A., Putirka, K., Pluhar, C.J., and Melosh, B.L., 2010, Birth of a plate bound-

- ary: Geological Society of America Abstracts with Programs, v. 42, no. 4, p. 80.
- Busby, C., Koerner, A.K., Melosh, B., Hagan, J.C., and Andrews, G.D.M., 2013a, Sierra Crest graben-vent system: A Walker Lane pull-apart in the ancestral Cascades Arc: *Geosphere*, v. 9, doi:10.1130/GES00670.1.
- Busby, C., Putirka, K., Renne, P., Melosh, B., Koerner, A., and Hagan, J., 2013b, A tale of two Walker Lane pull-aparts: Geological Society of America Abstracts with Programs, v. 45, no. 6, p. 59.
- Cashman, P.H., Trexler, J.H., Muntean, T.W., Faulds, J.E., Louie, J.N., and Oppliger, G.L., 2009, Neogene tectonic evolution of the Sierra Nevada–Basin and Range transition zone at the latitude of Carson City, Nevada, *in* Oldow, J.S., and Cashman, P.H., eds., Late Cenozoic structure and evolution of the Great Basin–Sierra Nevada transition: Geological Society of America Special Paper 447, p. 171–188, doi:10.1130/2009.2447(10).
- Curtis, G.H., 1951, The geology of the Topaz Lake quadrangle and the eastern half of the Ebbetts Pass quadrangle [Ph.D. thesis]: Berkeley, University of California, scale 1:125,000, 316 p., doi:oclc/21772219.
- Garside, L.J., Henry, C.D., Faulds, J.E., and Hinz, N.H., 2005, The upper reaches of the Sierra Nevada auriferous gold channels, *in* Rhoden, H.N., et al., eds., Window to the world: Geological Society of Nevada Symposium Proceedings 2005: Reno, Geological Society of Nevada, p. 209–235.
- Giusso, J.R., 1981, Preliminary geologic map of the Sonora Pass 15-minute quadrangle, California: U.S. Geological Survey Open-File Report OF-81-1170, scale 1:62,500.
- Hagan, J.C., 2010, Volcanology, structure, and stratigraphy of the central Sierra Nevada range front (California), Carson Pass to Sonora Pass [Ph.D. thesis]: Santa Barbara, University of California, publication 3398791, 267 p.
- Hagan, J.C., Busby, C.J., Putirka, K., and Renne, P.R., 2009, Cenozoic palaeocanyon evolution, Ancestral Cascades arc volcanism, and structure of the Hope Valley–Carson Pass region, Sierra Nevada, California: *International Geology Review*, v. 51, p. 777–823, doi:10.1080/00206810903028102.
- Henry, C.D., 2008, Ash-flow tuffs and paleovalleys in northeastern Nevada: Implications for Eocene paleogeography and extension in the Sevier hinterland, northern Great Basin: *Geosphere*, v. 4, p. 1–35, doi:10.1130/GES00122.1.
- Henry, C.D., and Perkins, M.E., 2001, Sierra Nevada–Basin and Range transition near Reno, Nevada: Two-stage development at 12 and 3 Ma: *Geology*, v. 29, p. 719–722, doi:10.1130/0091-7613(2001)029<0719:SNBART>2.0.CO;2.
- Henry, C.D., Hinz, N.H., Faulds, J.E., Colgan, J.P., John, D.A., Brooks, E.R., Cassel, E.J., Garside, L.J., Davis, D.A., and Castor, S.B., 2012, Eocene–Early Miocene paleotopography of the Sierra Nevada–Great Basin–Nevadaplano based on widespread ash-flow tuffs and paleovalleys: *Geosphere*, v. 8, p. 1–27, doi:10.1130/GES00727.1
- King, N.M., Hillhouse, J.W., Gromme, S., Hausback, B.P., and Pluhar, C.J., 2007, Stratigraphy, paleomagnetism, and anisotropy of magnetic susceptibility of the Miocene Stanislaus Group, central Sierra Nevada and Sweetwater Mountains, California and Nevada: *Geosphere*, v. 3, p. 646–666.
- Koenig, J.B., 1963, Geologic map of California: Walker Lane sheet: California Division of Mines and Geology, scale 1:250,000.
- Koerner, A.K., 2010, Cenozoic evolution of the Sonora Pass to Dardanelles region, Sierra Nevada, California: Paleochannels, volcanism and faulting [M.S. thesis]: Santa Barbara, University of California at Santa Barbara, 146 p.
- Koerner, A., Busby, C., Putirka, K., and Pluhar, C., 2009, New evidence for alternating effusive and explosive eruptions from the type section of the Stanislaus Group in the “cataract” paleocanyon, central Sierra Nevada (CA), *in* Ernst, G., ed., The Rise and Fall of the Nevadaplano: *International Geology Reviews*, v. 51, nos. 9–11, p. 962–985.
- Lebas, M.J., Lemaître, R.W., Streckeisen, A., and Zanettin, B., 1986, A chemical classification of volcanic-rocks based on the total alkali silica diagram: *Journal of Petrology*, v. 27, p. 745–750, doi:10.1093/petrology/27.3.745
- Lindgren, W., and Knowlton, F.H., 1911, The Tertiary gravels of the Sierra Nevada of California: U.S. Geological Survey Professional Paper 73, 226 p.
- Pluhar, C.J., Deino, A.L., King, N.M., Busby, C.J., Hausback, B.P., Wright, T., and Fischer, C., 2009, Lithostratigraphy, magnetostratigraphy, and radiometric dating of the Stanislaus Group, CA, and age of the Little Walker Caldera: *International Geology Review*, v. 51, p. 873–899, doi:10.1080/00206810902945017.
- Priest, G.R., 1979, Geology and geochemistry of the Little Walker volcanic center, Mono County, California [Ph.D. thesis]: Corvallis, Oregon State University, 311 p., doi:oclc/83332126.
- Putirka, K., and Busby, C.J., 2007, The tectonic significance of high K₂O volcanism in the Sierra Nevada, California: *Geology*, v. 35, p. 923–926, doi:10.1130/G23914A.1.
- Putirka, K.D., and Busby, C.J., 2011, Introduction: Origin of the Sierra Nevada and Walker Lane: *Geosphere*, v. 7, p. 1269–1272, doi:10.1130/GES00761.1.
- Ransome, F.L., 1898, Some lava flows on the western slope of the Sierra Nevada, California: U.S. Geological Survey Bulletin 89, 74 p.
- Renne, P.R., Balco, G., Ludwig, K.R., Mundil, R., and Min, K., 2011, Joint determination of ⁴⁰K decay constants and ⁴⁰Ar/³⁹K for the Fish Canyon sanidine standard, and improved accuracy for ⁴⁰Ar/³⁹Ar geochronology: Reply: *Geochimica et Cosmochimica Acta*, v. 75, p. 5097–5100, doi:10.1016/j.gca.2011.06.021.
- Renne, P.R., Deino, A.L., Hilgen, F.J., Kuiper, K.F., Mark, D.F., Mitchell, W.S., III, Morgan, L.E., Mundil, R., and Smit, J., 2013, Time scales of critical events around the Cretaceous–Paleogene boundary: *Science*, v. 339, p. 684–687, doi:10.1126/science.1230492.
- Riley, P., Tikoff, B., and Hildreth, W., 2012, Structural controls of contiguous but independent magmatic systems: Mono-Inyo craters, Mammoth Mountain and Long Valley caldera, California: *Geosphere*, v. 8, p. 740–751, doi:10.1130/GES00662.1.
- Schweickert, R.A., Lahren, M.M., Smith, K.D., and Karlin, R.D., 1999, Preliminary map of active faults of the Lake Tahoe basin: *Seismological Research Letters*, v. 70, p. 306–312, doi:10.1785/gssrl.70.3.306.
- Schweickert, R.A., Lahren, M.M., Karlin, R.D., and Howle, J., 2000, Lake Tahoe active faults, landslides, and tsunamis, *in* Lageson, D.R., et al., eds., Great Basin and Sierra Nevada: Geological Society of America Field Guide 2, p. 1–22, doi:10.1130/0-8137-0002-7.1.
- Schweickert, R.A., Lahren, M.M., Smith, K.D., Howle, J.F., and Ichinose, G., 2004, Transtensional deformation in the Lake Tahoe region, California and Nevada, USA: *Tectonophysics*, v. 392, p. 303–323, doi:10.1016/j.tecto.2004.04.019.
- Slemmons, D.B., 1953, Geology of the Sonora Pass region [Ph.D. thesis]: Berkeley, University of California, 201 p.
- Slemmons, D.B., 1966, Cenozoic volcanism of the central Sierra Nevada, California, *in* Bailey, E.H., ed., Geology of northern California: California Division of Mines and Geology Bulletin 170, p. 199–208.
- Stewart, J.H., and Carlson, J.E., 1978, Geologic map of Nevada: U.S. Geological Survey in collaboration with Nevada Bureau of Mines and Geology, scale 1:500,000.
- Surpless, B.E., Stockli, D.F., Dumitru, T.A., and Miller, E.L., 2002, Two-phase westward encroachment of Basin and Range extension into the northern Sierra Nevada: *Tectonics*, v. 21, p. 2–1–2–10, doi:10.1029/2000TC001257.
- Takarada, S., Ui, T., and Yamamoto, Y., 1999, Depositional features and transportation mechanism of valley-filling Iwasegawa and Kaida debris avalanches, Japan: *Bulletin of Volcanology*, v. 60, p. 508–522, doi:10.1007/s004450050248.
- Unruh, J.R., Humphrey, J., and Barron, A., 2003, Trans-tensional model for the Sierra Nevada frontal fault system, eastern California: *Geology*, v. 31, p. 327–330, doi:10.1130/0091-7613(2003)031<0327:TMFTSN>2.0.CO;2.
- Wagner, D.L., and Saucedo, G.J., 1992, Geologic map of the Chico Quadrangle: California Division of Mines and Geology, Regional Geologic Map 7A, scale 1:250,000.
- Wagner, D.L., Jennings, C.W., Bedrossian, T.L., and Bor-tugno, E.J., 1981, Geologic map of the Sacramento quadrangle, California, 1:250,000: California Division of Mines and Geology, Regional Geologic Map 1A, scale 1:250,000.
- Wakabayashi, J., and Sawyer, T.L., 2001, Stream incision, tectonics, uplift, and evolution of topography of the Sierra Nevada, California: *Journal of Geology*, v. 109, p. 539–562, doi:10.1086/321962.
- Whitney, J.D., 1880, The auriferous gravels of the Sierra Nevada of California: Harvard University Museum of Comparative Zoology Memoir 1, 659 p., doi:org/10.5962/bhl.title.65298.